JPRS-JST-94-009
5 MAY 1994

Foreign Broadcast Information Service

JPRS Report

Science & Technology

Japan

FINE CERAMICS: TRAIL AND ACCOMPLISHMENT OF NEXT-GENERATION R&D

JPRS-JST-94-009
5 MAY 1994

SCIENCE & TECHNOLOGY

JAPAN

FINE CERAMICS: TRAIL AND ACCOMPLISHMENT OF NEXT-GENERATION R&D

94FE0398/43070054 Tokyo FINE CERAMICS in Japanese/English Mar 93 pp 1-2133

[Selected articles and selected English abstracts from Next-Generation R&D Program on Fine Ceramics conducted by the Engineering Research Association for High-Performance Ceramics under contract with NEDO. Part of MITI's "Jisedai Project" (1981-93)]

CONTENTS

Objectives, Outline of Third Phase

94FE0398A Tokyo FINE CERAMICS in Japanese Mar 93 pp 3-8

[Text] When the complete plan was drawn at the beginning of the project, its third phase was designated as the verification phase for checking how close overall project achievements will have been made to established targets for technology development by using complex-shaped models which resemble the real components for separate applications. At that time, there were no limitations for application target devices, although from the middle of the second phase, when the electric power development special account budget was newly introduced, "ceramic gas turbine components for coal gasification compound generation systems" were designated to be the targets for verification. However, there was to be no change in the ground for the material technology development direction which had been the original objective of the next generation's industrial key technology R&D project. Therefore, the significance of establishing the specific targets was to develop systematic knowledge and technical know-how concerning the technology that could give guidelines which would always be capable of effectively solving technical problems concerning production and utilization of these turbine components beyond their verification tests. Needless to say, notable achievements in individual technology, have also been expected.

The designated gas turbine components were a stator (the stationary component: high corrosion and wear-resistance) and a rotor (the rotating component: high strength), both of which were regarded appropriate on the basis of their compliance to the research direction since the initiation of this project. After the judgment that the range and performance of materials that had been developed by the end of the second phase were insufficient against required use environment, the basic plan was modified to set the development targets as shown in Table 1 based on ideal performance values for ceramic gas turbine materials from the standpoint of turbine users. Thus, additional studies were initiated to further improve the performance of already developed materials, develop new high-toughness materials, develop surface reinforcement technology, and examine the mechanical shock fracture phenomenon. At the same time, the R&D project term was extended for two more years, so that the best suitable material can be selected from among developed materials, and verification tests can be carried out in the final extended period. In addition, further cooperation was promoted for the areas that had previously been stressed: the fusion of production process technologies and the compilation of strength data in connection with evaluation application

technologies. Based on the above, the research topics were shuffled for the third phase, as shown in Table 2.

Table 1. Target Performances for Third Phase

Field	Target value
Materials intended for use at temperatures above 1,400°C	(1) Instantaneous fracture strength: performance values given below must be satisfied in air and at a temperature above 1,400°C a. minimum guaranteed strength: 400 MPa b. rejection rate: less than 20% c. Weibull coefficient (reference value: more than 20 (2) Delayed fracture strength: performance values given below must be satisfied in 10,000-hour creep tests in air at a temperature above 1,400°C: creep strength: more than 250 MPa (3) Oxidation, corrosion and wear resistance: neither significant strength change nor material deterioration should occur after being left standing for more than 200 hours in a flow of coal ash-containing combustion gas at 1,400°C or higher. (4) Fracture toughness value: materials that can satisfy all the above conditions must further satisfy the following value in tests of room temperature: fracture toughness value: more than 8 MPam$^{1/2}$
Materials intended for use at temperatures above 1,250°C	(1) Instantaneous fracture strength: performance values given below must be satisfied in air and at a temperature above 1,250°C a. minimum guaranteed strength: 600 MPa b. rejection rate: less than 20% c. Weibull coefficient (reference value: more than 20 (2) Delayed fracture strength: performance values given below must be satisfied in 10,000-hour creep tests in air at a temperature above 1,250°C: creep strength: more than 250 MPa (3) Oxidation, corrosion and wear resistance: neither significant strength change nor material deterioration should occur after being left standing for more than 200 hours in a flow of coal ash-containing combustion gas at 1,250°C or higher. (4) Fracture toughness value: materials that can satisfy all the above conditions must further satisfy the following value in tests of room temperature: fracture toughness value: more than 15 MPam$^{1/2}$

Table 2. Research Topics in Third Phase

1. Elemental technology development for turbine components
   (1) Model design, and test/evaluation
   (2) Material design
      a) Silicon nitride
      b) Silicon carbide
   (3) Molding, sintering
      a) Silicon nitride
      b) Silicon carbide
   (4) Machining
   (5) Bonding
      a) Silicon nitride
      b) Silicon carbide
   (6) Guarantee tests
2. Material technology development
   (1) Toughness reinforcing materials
      a) Grain-dispersed high-toughness materials
      b) Fiber-reinforced high-toughness materials
      c) Crystallization-controlled high-toughness materials
   (2) Surface strengthening technologies
      a) Surface modification strengthening technology
      b) Surface coating strengthening technology
3. Evaluation technologies
   (1) Nondestructive inspection
   (2) Design standards
   (3) Fracture factor analysis
      a) Fracture under tensile compound stress
      b) Fracture under stress gradient
      c) Impact fracture
      d) Corrosion/fracture in high-temperature environment
      e) Thermal fatigue fracture

The target values listed in Table 1 are the ultimate performances for turbine materials. It was anticipated to be extremely difficult to simultaneously satisfy these conditions in the extended research period because both material and technology development had to be completely merged. Therefore, based on studies by the promotion and evaluation committees, it was decided, for the time being, to carry out separately but simultaneously the development of monolithic materials and the development of toughness reinforcement materials. As a result, the third phase targets for the research topics, shown in Table 2, concerning elemental technology development and material technology development for turbine components were established as shown in Tables 3 and 4. Included in these targets were the expected-to-achieve technology target levels that had not been a part of the basic plan concerning machining, surface reinforcement and bonding technologies which were classified as related technologies. Furthermore, although it was difficult to do quantitatively, target values were set for evaluation/application technology-related research items, as shown in Table 5 [not reproduced].

Table 3. Elemental Technology Development for Turbine Components

	Silicon nitride	Silicon carbide	Remarks
Model design·Test/evaluation	Design, tests and analyses of secondary and compromise models		•Also aims at achieving silicon carbide targets with silicon nitride
Material design	Verify strengths of rotor-corresponding compromise models and cut testpieces with rotation fracture tests: instantaneous fracture: ≥600 MPa (1,250°C) delayed fracture: ≥250 MPa (10,000 h) fracture toughness: K_{IC}≥6 MPa·m$^{1/2}$	Verify strengths of stator-corresponding compromise models and cut testpieces with heat-shock fracture tests: instantaneous fracture: ≥400 MPa (1,400°C) delayed fracture: ≥250 MPa (10,000 h) fracture toughness: K_{IC}≥3 MPa·m$^{1/2}$	
Molding/sintering	Verify strengths of rotor-corresponding compromise secondary models and cut test-pieces with rotation fracture tests: instantaneous fracture: ≥600 MPa (1,250°C) delayed fracture: ≥250 MPa (10,000 h) fracture toughness: K_{IC}≥6 MPa·m$^{1/2}$	Verify strengths of stator-corresponding compromise secondary models and cut test-pieces with heat-shock fracture tests: instantaneous fracture: ≥400 MPa (1,400°C) delayed fracture: ≥250 MPa (10,000 h) fracture toughness: K_{IC}≥3 MPa m$^{1/2}$	
Machining	•Grinding ratio of more than 6,000 and strength loss by test material of less than 15 percent at grinding efficiency of 100 mm^3/mm·sec •Surface roughness: 0.3 μm Ra •Dimensional precision: 5 μm •Machined surface properties: hardness variation less than ±5 percent, residual compression stress		•Flat surface grinding
Bonding	C-C: 80 percent of matrix at 1,250°C C-M: 200 MPa at 400°C; residual strength of 80 percent after 1,000 repetitions of temperature increase and decrease between room temperature and 400°C	C-C· 80 percent of matrix at 1,400°C C-M: 200 MPa at 500°C; residual strength of 80 percent after 1,000 repetitions of temperature increase and decrease between room temperature and 500°C	•Bonded area is 10 mm φ

Notes: 1. Target strength values were set by the basic plan, except fracture toughness values are to be maintained at least at the same level as that of existing materials.

2. R&D targets for guarantee tests are included in the classification of evaluation/application technologies.

Table 4. Material Technology Development

	Silicon nitride matrix	Silicon carbide matrix
Particle-dispersed high-toughness materials	$K_{IC} \geq 12$ MPa·m$^{1/2}$ $\sigma_{1250} \geq 600$ MPa	$K_{IC} \geq 7$ MPa·m$^{1/2}$ $\sigma_{1400} \geq 400$ MPa
Fiber-reinforced high-toughness materials	$K_{IC} \geq 15$ MPa·m$^{1/2}$ $\sigma_{1250} \geq 500$ MPa	$K_{IC} \geq 8$ MPa·m$^{1/2}$ $\sigma_{1400} \geq 300$ MPa
Crystal-controlled high-toughness materials	$K_{IC} \geq 2 \times K_{IC}$ for each component phase alone (minimum value: 12 MPa·m$^{1/2}$) $K_{IC} \geq \sigma 1250$ for each component phase alone (minimum value: 400 MPa)	
Surface modification technology	•Oxidation resistance (1,000~1,400°C) (30 percent higher than that of base material) •Wear resistance (one-digit higher than that of base material)	•Oxidation resistance (1,000~1,400°C) (equal to or higher than that of base material) •Wear resistance (one-digit higher than that of base material)
Surface coating technology	•Oxidation resistance (1,000~1,400°C) (30 percent higher than that of base material) •Wear resistance (one-digit higher than that of base material)	•Oxidation resistance (1,000~1,400°C) (equal to or higher than that of base material) •Wear resistance (one-digit higher than that of base material)

1. As a rule, testpieces of high-toughness materials are test blocks of 100 x 50 x 10~15 mm thick and smaller pieces cut from one of the blocks.
2. Substrates used for the evaluation of surface-reinforcing materials are those materials developed by a corporation in charge of that section of research.
3. Methods for measuring oxidation and wear resistance are to follow the methods used in the molding/sintering section in the second phase.

Under the above-described plan, another set of objectives of the research activities in the third phase included the following: the design of monolithic materials appropriate for sophisticated targets to be achieved, the design, production and testing of secondary models (Figure 1) for the gas turbine stator and rotor with the shapes and stress elements to be tested for the final verification; the development of basic conditions for machining and bonding that would also be applicable to the final models; and the development of nondestructive inspection and guarantee test methods for the models. As a result of material design studies, silicon nitride made by the two-stage sintering method was added to two types of silicon carbide, which had been sintered with different sintering additives, to be candidates for the 1,400°C stability-required stator model material, and all three materials were to be examined in a parallel manner through the final verification. For the rotor model, only the original high-strength silicon nitride was to be verified. In addition based on various, more current ideas, toughness-reinforcing materials for both silicon nitride and silicon carbide matrices were developed, and supplementary studies concerning the surface reinforcement technology were carried out.

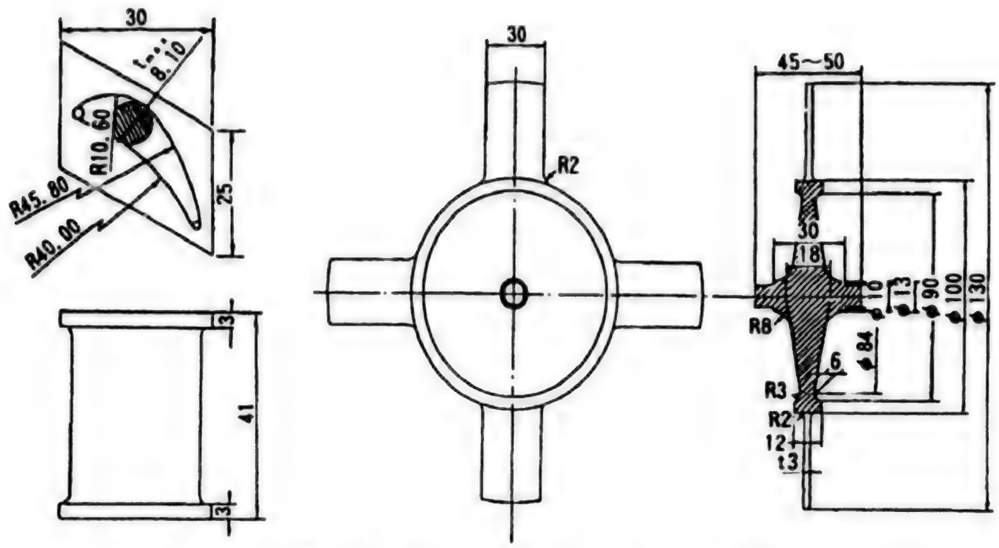

Figure 1. Secondary Models (Left: Stator; Right: Rotor)

Although various secondary stator models, when tested at the end of the phase, satisfied the necessary requirements for heat shock resistance, the secondary rotor model fractured in the high-temperature rotation test with approximately 85 percent of the target strength of 600 MPa. Since cut-out testpieces had achieved the target value for instantaneous fracture strength, the model fracture must have been caused by its lack of uniformity due to plural shape elements with a large effective volume. Incidentally, the delayed fracture strength and the corrosion resistance of various models will be evaluated in the integrated technology R&D phase.

In the toughness reinforcing material research project that had been initiated as a supplementary project, toughness reinforcing materials were developed under the headings of particle-dispersed, fiber-reinforced and crystal-controlled in a parallel fashion. However, by the end of the third phase, none of the materials achieved the target fracture toughness value with a balance with strength and corrosion resistance. Thus, the research will be continued into the integrated technology R&D phase with emphasis on material search and clarification of correlation between structure and properties. As a result, it was decided to test only monolithic materials at the final verification tests. Incidentally, the three research topics under the toughness reinforcing material development and the surface modification reinforcement technology by the ion implantation method were discontinued at the completion of their basic study phases due to their scales of both work involved and outlay.

Looking over the individual research topics, attention-worthy achievements were made in particular in the application of thermosetting resin as a part of the development of the complex-shape injection molding technology, the remarkable improvements in corrosion and friction resistance by the chemical vapor deposition method, and the expansion of material strength data.

Section 1. Fundamental Technology Development for Coal Gasification Ceramic Gas Turbine

Chapter I. Research: Third Phase (1989-1993)

2. Design for Components of Turbine Model

43070054A Tokyo FINE CERAMICS in English Mar 93 p 10

[English abstract of article by T. Mikami, K. Tagashira, K. Katoono, and J. Okamura Ishikawajima-Harima Heavy Industries Co., Ltd.]

[Text] As a first model of this project, hitherto ceramic cylindrical model for thermal shock test and simple shape disk model for the hot spin test have been conducted. Through the tests, the evaluation method of ceramic components was established.

Following these research works, as an element of coal gasifier gas turbine, corresponding complicated and larger ceramic blade and nozzle models were designed and tested according to the project targets with respect to the strength.

The models which are named second models, are made by monolithic silicon nitride or silicon carbide. The nozzle model was examined by thermal shock tests while the blade model was by hot spin testing. These test results were compared with the strength of test specimens. Results are finally reflected on the material design, forming and sintering process of the ceramics. Also through this program, an evaluation method of ceramic components is to be established. The results are;

(1) Most nozzles cleared the target value even after applying higher stress than the target value. This is supposed to be very small effective volume of the model. Especially nozzles with silicon nitride showed no failure. This is due to material properties such as lower thermal expansion and Young's modulus.

(2) Blade models showed lower strength than expected. Contrary to the nozzle, effective volume of the blade model is higher than that of the nozzle. Therefore, failure probability of the blade is much higher than the nozzle model. Blade and nozzle combined rig tests are going to be held as a next program.

3. Monolithic Materials Design

3.1 Post-Sintered Si_3N_4

43070054B Tokyo FINE CERAMICS in English Mar 93 p 26

[English abstract of article by Yoshio Hayashi, Yoshiro Noda, Toru Shimamori, Masakazu Watanabe, and Yasushi Matsuo, R&D Center, NGK Spark Plug Co., Ltd.]

[Text] In the first and second phases of the fine ceramics project, post-sintered Si_3N_4 ceramics with good oxidation resistance at 1300°C were investigated. In the third phase, post-sintered Si_3N_4, ceramics with high strength, high creep resistance at 1400°C have been investigated. Post-sintering was carried out by hot-pressing and sinter-HIPing. To improve high temperature properties, investigations of sintering additives and sintering conditions were carried out in this study. It was found that ionic radius of rare-earth elements have a great influence on high-temperature properties, and that the microstructure of post-sintered Si_3N_4 has a great influence on the flexural strength at room temperature [R.T.] and 1400°C. In this study, post-sintered Si_3N_4, doped with Sc_2O_3 and [Sc_2O_3 + Y_2O_3 which performance exceeded the target of the third phase was developed. For post-sintered Si_3N_4 doped with Sc_2O_3, 1400°C strength, Weibull modulus and fracture toughness were 451MPa, 20 and 5MPa·m$^{1/2}$, respectively. For post-sintered Si_3N_4 doped with [Sc_2O_3 + Y_2O_3], 1400°C strength, Weibull modulus and fracture toughness were 601MPa, 20 and 6MPa·m$^{1/2}$, respectively.

3.2 Monolithic Material Design of Silicon Nitride Ceramics

43070054C Tokyo FINE CERAMICS in English Mar 93 p 40

[English abstract of article by Tomoyuki Awazu, Yoshishige Takano, Hisao Takeuchi, Osamu Komura, and Masaya Miyake, Itami Research Laboratories, Sumitomo Electric Industries, Ltd.

[Text] Since silicon nitride is fabricated using liquid phase sintering, sintering additives usually remain between Si_3N_4 grains as grain boundary phases. The grain boundary phases are softened and suddenly reduce the strength of sintered body under high temperature. This phenomenon occurs more notably when grain boundary phases contain glassy ones. The condition of grain boundary phases also influences the creep property under high temperature. This paper investigates the internal friction of Si_3N_4 sintered body, which relates to grain boundary slip and diffusion of atoms. This investigation will clarify the relationship between the conditions of grain boundary phases (ex. crystallization) and the internal friction changes. The creep properties of the sintered body are also studied by analyzing the results of internal friction measurements. This will allow us to fully consider the relationship between the composition of sintering additives and the effects of heat treatment for crystallization.

3.3 Development of Monolithic Silicon Carbides With Addition of Alumina

43070054D Tokyo FINE CERAMICS in English Mar 93 p 53

[English abstract of article by Takashi Kanno, Nobuhiro Shinohara, and Keiichiro Suzuki, Asahi Glass Co., Ltd., Research Center]

[Text] Densification behavior and mechanical properties of silicon carbide ceramics with the addition of alumina were investigated for two types of silicon carbide powders developed by Showa Denko Co., Ltd. The result of pressureless sintering for both powders demonstrated that the densification behavior could be classified into three stages;

1) First stage (1700-1800°C)

Slight densification by the reconstruction of silicon carbide particles

2) Intermediate stage (1800-1900°C)

Formation of the viscous phase including an added alumina component, and rapid densification resulted from the reconstruction and mass transport (solution-precipitation) mechanisms through this second phase

3) Final stage (>1900°C)

Slow densification with the growth of plate-like grains.

HIPing was effective for further densification, and the samples consisted of densely packed, plate-like grains in jigsaw pattern after HIPing.

Mechanical properties were evaluated for testpieces cut from the test block of 100 x 50 x 15 mm. Thermal shock tests were also carried out at IHI for "stator vane models" to confirm the performance of HIPed silicon carbides with addition of alumina. The results were as follows;

(1) Flexural strength: σ_{3P} = 607MPa (1400°C) with Weibull modulus: m = 23.4 was obtained by three-point bending tests. Minimum guaranteed strength, fast-fracture strength of failure probability of 20% estimated for effective volume of stator vane model (V_{ϵ} = 2.1mm^3), was evaluated as σ_f(20%) = 532MPa (1400°C).

(2) Creep rupture strength: $\sigma_{4P} \geq$ 250MPa (1400°C-1,000h) was obtained by four-point bending test.

(3) Fracture toughness: K_{IC} = 4.6MPam$^{1/2}$ was achieved by the single-edge precracked beam (SEPB) method.

(4) All the stator vane models (n=9) survived the thermal shock tests under the thermal stress of 490~568MPa except for one case which ruptured at 510MPa. Including one case which broke down at 510MPa, all the vane models were confirmed to overcome the target value of ≥ 400MPa.

3.4 Fracture Toughness of Silicon Carbide Materials

43070054E Tokyo FINE CERAMICS in English Mar 93 p 69

[English abstract of article by Kazunori Koga, Masaki Kaji, and Shoji Kohsaka, Central Research Laboratory, Kyocera Corporation]

[Text] A mechanism of enhancement of fracture toughness is discussed based on the compressive residual stress in silicon carbide materials sintered with B-C addition. The compressive stress in silicon carbide matrix and the fracture toughness increases with an increasing amount of TiB_2 addition. A linear relationship was found between the compressive stress in silicon carbide matrix and the fracture toughness of the composite. This result was successfully applied to increase the fracture toughness of the silicon carbide by origination of residual stress from anisotropic characteristics in thermal expansion coefficient of polymorphs.

4. Sintering Forming

4.1 Development of Silicon Nitride Second Stage Rotor Model

43070054F Tokyo FINE CERAMICS in English Mar 93 p 81

[English abstract of article by K. Nishida, T. Kameda, T. Suto, S. Inada, A. Tsuge, and Y. Goto, Toshiba Corp.; and T. Kanda, T. Tatsuno, and T. Takebe, Kobe Steel, Ltd.]

[Text] For the fabrication of the silicon nitride second stage rotor model, process containing injection molding and capsule-free HIPing was introduced. The injection molding process has difficulty in obtaining defect-free, dewaxed moldings with thick portion of, especially, more then 10mm. The reason is thought to be that at a temperature of organic binder removal, strength of molded shape is almost zero, and it is not able to withstand gas pressure due to evaporation or decomposition of organic binder, and then cracks. To overcome the default, thermosetting organic binder system was investigated. The system consists of low temperature evaporating ingredient and strength-bearing thermosetting ingredient. From the results of strength measurement at 200°C on various ceramic/organic binder compositions, it became clear that a structure model consisting of thermosetting resins precipitated around the ceramic powder and connected with each other to form a three-dimensional skeleton of thermosetting resin/ceramic powder gave most fruitful results after binder removal. The HIP process, HIP temperature and gas composition were investigated to optimize as-HIP surface properties. HIP temperature of 1800°C and gas composition of 2%-nitrogen/98%-argon were selected as HIP conditions for fabrication of the model. Under these process conditions, the rotor models were fabricated and gave satisfactory strength level on the test pieces cut from it.

4.2 Development of Stator Models by Injection Molding of Silicon Carbide With the Addition of Alumina

43070054G Tokyo FINE CERAMICS in English Mar 93 p 92

[English abstract of article by Takashi Kanno and Nobuhiro Shinohara, Asahi Glass Co., Ltd., Research Center]

[Text] The stator model for ceramic gas-turbine has been developed with monolithic silicon carbides through "injection molding" plus "pressureless sintering" plus "HIPing" processes by use of β-SiC powders with sintering aid of 5wt% alumina. The 52.5vol% of silicon carbide powders with alumina were compounded with binder (polyethylene and polystyrene) by addition of a plasticizer (octyl palmitate) and lubricant (stearic acid and stearyl alcohol) to achieve uniform dispersion of powders in polymer melts.

The dimensional accuracies were evaluated for as-molded, pressureless sintered, and HIPed stator models with respect to the coefficient of variation among the separate stator models. Except for the curvature in the stator vane, the coefficient of variation was controlled to less than 0.2%. Average linear-shrinkage of 20.12% resulted with a standard deviation of 0.11% and the coefficient of variation of 0.53% for the HIP'ed stator models of the bulk density of 98.06%TD.

The mechanical properties of the stator models were evaluated with testpieces cut from the shroud of the stator models and eventually the performance of the stator models was confirmed by thermal shock tests at IHI.

(1) Flexural strength: σ_{3P} = 525MPa (1400°C) with Weibull modulus: m = 17.3 was obtained by three-point bending tests. A minimum guaranteed strength, defined in this project as fast-fracture strength of failure probability, of 20% estimated for effective volume of the stator model (V_ϵ = 3.2mm^3), was evaluated as σ_T (20%) = 448MPa (target value ≥ 400MPa at 1400°C).

(2) Creep rupture strength: σ_{4P} ≥ 250MPa (1400°C-1,000h) was obtained by four-point bending test at 1,000h (target value ≥ 250MPa at 1400°C for 10,000h).

(3) Fracture toughness: K_{IC} = 6.5MPam$^{1/2}$ was achieved by the single-edge precracked beam (SEPB) method (target value ≥ 3MPam$^{1/2}$).

(4) All the stator models (n=10) were confirmed to survive the thermal shock tests under the thermal stress of 510~608MPa.

5. Processing Technology

5.1 Development of High-Efficiency Machining for Silicon Nitride

43070054H Tokyo FINE CERAMICS in English Mar 93 p 117

[English abstract of article by Masahiro Okamoto, Yasuo Niino, and Hideki Nagano, Toyoda Machine Works, Ltd.]

[Text] The high efficiency grinding of silicon nitride is carried out to make the following clear.

The grinding at the efficiency of $100 mm^3/mm \cdot s$ and with the grinding ratio of 6000 can be realized, using a high-rigidity, high-precision grinding machine together with a strong grinding wheel. In this case, minute cracks may be created on the workpiece surface to cause decreases in strength. This can be effectively avoided by removing heat during grinding.

The recovery of strength can be made by irradiating a laser beam onto the surface of the workpiece which has been decreased in strength.

5.2 Compound Plasma Grinding

43070054I Tokyo FINE CERAMICS in English Mar 93 p 118

[English abstract of article by Masaaki Ishiyama, Inoue Japan Research Inc.]

[Text] Grinding fine ceramics on an ordinary grinding machine with the aid of plasma, an electrolyte of 3% sodium hydroxide flushed, plasma discharge is produced by considerably high voltage applied between the grinding wheel and workpiece with subsidiary electrodes which are isolated from the machine body.

By thermal shock and discharging pressure generated by plasma discharge the workpiece surface becomes so fragile that it can be ground off by ordinary mechanical grinding. The grinding machine used requires no special high rigid construction.

As the experimental result, the grinding power consumption is reduced by approximately 30% compared with the ordinary grinding method and the installation cost is approximately one-third that of laser compound grinding. Further it has been discovered that the material toughness which was reduced by machining strain is restored by continuous heating by plasma.

6. Joining Technology

6.1 Joining of Silicon Nitride Ceramics

43070054J Tokyo FINE CERAMICS in English Mar 93 p 147

[English abstract of article by Hisao Takeuchi, Yoshishige Takano, Akira Yamakawa, and Masaya Miyake, Sumitomo Electric Industries, Ltd., Itami Research Laboratories]

[Text] We have investigated joinings of Si_3N_4-Si_3N_4 and Si_3N_4-metal for the application at high-temperature imaging of a ceramics gas turbine.

For the joining of Si_3N_4-Si_3N_4, we developed processes consisting of non-pressure joining with joining pastes of Y_2O_3-Al_2O_3-SiO_2 mixed powder followed by HIPing. Maximum bending strength at 1250°C was 640MPa corresponding to 82% of Si_3N_4 itself.

For the joining of Si_3N_4-metal, we developed a process consisting of the multilayer metallization and brazing, especially attaching importance to heat-cycle resistance. Heat-cycle resistance was improved by use of interlayers for thermal stress reduction based on both gradation of thermal expansion coefficients (tungsten carbide based alloy, etc.) and plastic deformation (Ni), and brazing alloy (Au-Ni) with superior oxidation resistance. Flexural strength after 1,000 times heat cycle test between room temperature (RT) and 400°C in air was about 400MPa in which existed no reduction before the heat cycle.

6.2 Joining of Silicon Carbide

43070054K Tokyo FINE CERAMICS in English Mar 93 p 162

[English abstract of article by Kazunori Koga, Saburo Nagano, Syoji Kohsaka, Syuichi Tateno, and Masaki Terazono, Central Research Laboratory, Kyocera Corporation]

[Text] A silicon carbide sintered with B-C addition was joined by solid state diffusion using glass-sealed HIPing. The joined area was as large as 60mm in diameter. The flexural strength of the joined part was 500MPa which was more than 80% of that of the base material.

The joining between silicon carbide and SCM steel was carried out by reducing the residual stress in the silicon carbide due to the thermal expansion mismatch between them. Adjusting the thermal expansion coefficient of the insert materials between silicon carbide and SCM, successfully achieved the joining with a flexural strength of 300MPa.

The joining strength at 500°C after 1,000 times heat cycle test between room temperature and 500°C retained more than 80% of the initial one.

7. Particle Dispersion High-Toughness Materials

7.1 Improvement of Particulate-Reinforced Silicon Nitride Materials

43070054L Tokyo FINE CERAMICS in English Mar 93 p 176

[English abstract of article by Akio Yoshida, Miyuki Nakamura, Kei Isozaki, and Yukihiko Nakajima, Denki Kagaku Kogyo Co., Ltd., Omuta Plant]

[Text] The purpose of this research is to develop particulate-reinforced Si_3N_4 materials which can satisfy the target values of $K_{IC} \geq 12MPam^{1/2}$ and $\sigma_{1250^{\circ}C} \geq 600MPa$. The toughening mechanisms by the dispersion of some kinds of particulate and the use of hybrid (composite) powders were investigated. The obtained results are summarized as follows.

The fracture toughness of Si_3N_4–TiN sintered bodies having the large difference of thermal expansion between the matrix grain and dispersing particulate were largely influenced by the particle size and added amount of TiN. The maximum value of fracture toughness was $9.3MPam^{1/2}$ at 30wt% TiN addition.

According to the low oxidation resistance, the optimum amount of TiN was 5wt%. The Si_3N_4–TiN hybrid powders could be synthesized by the vapor phase reaction using CO_2 laser. The mechanical properties of sintered bodies made from the hybrid powders were $K_{IC} = 7.5MPam^{1/2}$ and $\sigma_{1250^{\circ}C} = 700MPa$ which were higher than those of the mixing powders.

The fracture toughness of Si_3N_4–SiC sintered bodies having little difference of thermal expansion between the matrix grain and dispersing particulate did not increase so much by SiC particle additions. Besides, the synthesis of nano-dispersed hybrid powders was confirmed. Many nano-sized SiC particles were present in an Si3N4 particle, so the mechanical properties of sintered bodies made from the hybrid powders were $K_{IC} = 7.8MPam^{1/2}$ and $\sigma_{1250^{\circ}C} = 730MPa$ which were higher than those of the mixing powders.

In the case of Cr_3C_2 dispersed particle, it accelerated the grain growth of matrix Si_3N_4. According to this effect, it was found that the fracture toughness of Si_3N_4–Cr_3C_2 sintered bodies were improved even by small additions of it. Although the improvements of the fracture toughness by the effects of the particulate dispersions, especially the hybrid powders, were confirmed to some extent, the target values could not be achieved. The microstructure control of sintered bodies was thought to be also important in order to toughen the particulate-reinforced Si_3N_4 materials.

7.2 Silicon Carbide Matrix

43070054M Tokyo FINE CERAMICS in English Mar 93 p 190

[English abstract of article by Hiroshi Hashegawa, Kagetaka Ichikawa, and Masataka Yamamoto, Showa Denko K.K.]

[Text] SiC-TiC composite powders (TiC10-40vol%) was produced by chemical vapor deposition (CVD) using $(CH_3)_2SiCl_2$ and $TiCl_4$ as source gases. The above mentioned powders (composite powders) were hot-pressed at 2100°C under two sets of temperature conditions (approximately 0.3°C/sec:HP and 30°C/sec:PAS). Mixed powders of commercially available SiC and TiC powders (mixed powders, TiC0-40vol%) were also hot-pressed under the same conditions.

The fracture toughness (K_{IC}) of the bodies produced by each composite powder and mixed powder by the two kinds of sintering methods was measured by the indentation fracture (IF) method. As a result, it was found that the K_{IC} of the body produced by each powder was highest at about TiC30vol% regardless of the sintering method, and that the maximum K_{IC} ($\sim$6.6MPa·$m^{1/2}$) of the body produced by the composite powder was about 30% higher than the maximum K_{IC} ($\sim$5.0MPa·$m^{1/2}$) of the body produced by the mixed powder.

The structures of the bodies were investigated. As a result, the following was found. TiC grains in the body produced by the composite powder exhibited similar growth to the grains within the body produced by the mixed powder, and a carbon rich phase of less than 10 nm width existed in the grain boundary of only the body produced by the composite powder. It was considered that the existence of the grain boundary phase caused a higher K_{IC}.

7.3 Particle Dispersion Toughened Boron-Doped Silicon Carbide

43070054N Tokyo FINE CERAMICS in English Mar 93 p 201

[English abstract of article by Goro Saiki, Industrial Property Corporation Center; Jiro Kondo, Tetsuro Nose, Shigeharu Matsubayashi, and Hiroshi Kubo, Advanced Materials and Technology Research Laboratories, Nippon Steel Corporation; Matsuo Maki, Environmental Plant Division, Nippon Steel Corporation; and Tadashi Ikemoto, Process Technical Research Laboratories, Nippon Steel Corporation]

[Text] The mechanical properties of MoB_2 particle dispersed boron-doped silicon carbide has been investigated. Using the hybrid-plasma reaction method, SiC-MoB_2 composite powders were synthesized. It was found that the sintered bodies from those powders had a lower density than that of mechanically mixed commercial powders. Oxidation and creep tests were carried out on the same samples. As a result, the oxidation rate was reduced and less degradation of mechanical properties were observed after the oxidation test. Creep rate was also reduced for the materials which had been prepared from the hybrid-plasma produced powders compared to those formed from mechanically mixed powders. The creep resistance was further improved in heat-treated samples with typical creep rate values between $8x10^{-7}$~$5x10^{-8}$ S^{-1} in the stress range 150~300MPa at 1773K.

7.4 MoB_2 Particulate-Reinforced SiC

43070054O Tokyo FINE CERAMICS in English Mar 93 p 213

[English abstract of article by Hiroshi Kubota and Shumei Hosokawa, Krosaki Corporation]

[Text] A fabrication process for forming particulate-reinforced SiC composites has been studied from fundamental viewpoints including pressureless sintering, HIP, and heat treatment. Target properties, for fracture toughness $K_{IC} \geq 7MPam^{1/2}$ and flexural strength σ 1400 ≥ 400MPa were not realized. However, a new fabrication process of $SiC-MoB_2$ composites has been developed, Compacts of $SiC-Mo_2B_5-MoB-B-C$ powder mixtures were sintered above 2100°C in an argon atmosphere. During the sintering process the following reaction took place between 1600 and 1800°C.

$$Mo_2B_5 + MoB \rightarrow 3MoB_2$$

The synthesis of MoB_2 was completed before the start of SiC matrix densification. Compared to monolithic SiC, the fracture toughness of the composites containing 15vol% MoB_2 increased 1.6 to 1.9 times when commercially available β-SiC powder was used and 2.7 times when boron-doped SiC powder was used. The fracture toughness of $SiC-MoB_2$ composites increased with increasing MoB_2 grain size and growth of rod like SiC grains.

8. Fiber-Reinforced High-Toughness Materials

8.1 Development of SiC Whisker-Reinforced Si3N4 Matrix Composites

43070054P Tokyo FINE CERAMICS in English Mar 93 p 227

[English abstract of article by Takayuki Fukasawa, Yasuhiro Goto, Toshiaki Mizutani, and Akihiko Tsuge, Toshiba Corporation, R&D Center]

[Text] SiC whisker-reinforced Si3N4 has been investigated to improve fracture toughness and high-temperature mechanical properties. The relationship between fracture toughness and process parameters, e.g., sintering temperature and sintering additives, were studied to optimize the effect of whisker. Consequently, research regarding control techniques of whisker orientation, optimization of matrix sintered at low temperatures, and evaluation and control of whisker/matrix interfaces have been performed. In this study, development of whisker-orientation control techniques by extrusion molding, effects of whisker on high-temperature creep behavior, measurement method and results of interfacial shear strength between fiber and matrix, and high-resolution observation of whisker matrix interfaces are reviewed.

8.2 Study on Fabrication Process of SiC Whisker-Reinforced SiC Ceramics

43070054Q Tokyo FINE CERAMICS in English Mar 93 p 248

[English abstract of article by Kaoru Miyahara, Takashi Sugita, Takashi Watanabe, Makoto Ohno, Shin Koga, and Tadashi Sasa, Research Institute, Ishikawajima-Harima Heavy Industries Co., Ltd.]

[Text] A fabrication process of SiC whisker-reinforced SiC ceramics has been developed, in consideration of microstructure of the materials, i.e. whisker/matrix interface, homogeneous whisker dispersion, orientation of whiskers, and possible whisker degradation during sintering.

Chemical vapor deposition (CVD) coating on whiskers was carried out to control a whisker/matrix interface. Carbon-coating was confirmed to bring about remarkable pull-out of whiskers on the fracture surface. For the purpose of the uniform mixture of powder and whiskers, a dispersion technique using ultrasonic irradiation was adopted. As a forming process, slurry-pressing was studied. Density of the slurry-pressed compacts were considerably affected by the morphology and the concentration of whiskers. Relatively dense compacts were obtained with whiskers of lower aspect ratio. Whiskers in the compacts were found to have preferred orientation perpendicular to the pressing axis. Furthermore, the extrusion process was also studied to obtain unidirectional orientation of whiskers. In this method, compacts were fabricated by stacking the extruded sheets containing whiskers. Densification was carried out by HIP using a glass container. To prohibit possible degradation of the whiskers at high temperatures, sinterability of the composites doped with several sintering additives was investigated at lower temperature. Highly dense composites were obtained by HIPing at 1750°C with 5% alumina addition.

8.3 Stacking Structure of Ceramics

43070054R Tokyo FINE CERAMICS in English Mar 93 p 264

[English abstract of article by Jin-Joo Matsui, Yoshishige Takano, Osamu Komura, Akira Yamakawa, and Masaya Miyake, Sumitomo Electric Industries, Ltd., Itami Research Laboratories]

[Text] In order to strengthen and toughen Si_3N_4 ceramics by addition of SiC-whiskers, we tried the control of interfacial properties between whisker and matrix and of orientation of whiskers. For interfacial control, the effects of Al_2O_3, ZrO_2, and carbon coating to the surface of whiskers were studied. The flexural strength and the fracture toughness of Si_3N_4 composite containing Al_2O_3-coated whiskers by decomposition of aluminum stearate, were stronger (1107MPa)and larger ($10.2 MPa \cdot m^{1/2}$)than those of the composite with non-coated whiskers. Transmission electron microscope (TEM) observation revealed that Al_2O_3-coated whiskers in the composite had a smoother surface than non-coated whiskers and that a film-layer was formed at the interface between whisker and matrix. For orientation control, the flexural strength and the creep rupture resistance at 1250°C of Si_3N_4 composite, reinforced with unidirectionally-oriented whiskers by the doctor-blade method, were much stronger (1180MPa) and much larger than those of monolithic Si_3N_4 ceramics. After creep testing, the new stacking fault and dislocation in the whiskers were observed by TEM. On the basis of these results, the mechanisms of toughening and high-temperature strengthening of $SiC(w)/Si_3N_4$ have been discussed.

8.4 Preformed CVI Silicon Carbide

43070054S Tokyo FINE CERAMICS in English Mar 93 p 281

[English abstract of article by Kazunori Koga, Masahide Akiyama, and Makoto Watanabe, Central Research Laboratory, Kyocera Corporation]

[Text] Three-dimensionally woven silicon carbide fiber was chemical vapor infiltrated (CVI) with dense silicon carbide at high temperatures. The interface between fibers and matrix is important to get a high fracture toughness. The precoating of carbon on the surface of silicon carbide fiber was essential for the pull-out of the fibers during fracture. The CVI silicon carbide composite material showed the fracture toughness of $15 MPa \cdot m^{1/2}$ and three-point flexural strength of 300MPa.

The temperature gradient was simulated to get a uniform and dense infiltration.

9. High-Toughness Ceramics With Controlled Crystalline by Unidirectional Solidification Method

43070054T Tokyo FINE CERAMICS in English Mar 93 p 294

[English abstract of article by Takashi Kanno, Yutaka Segawa, and Shigemi Katori, Asahi Glass Co., Ltd., Research Center]

[Text] Development of high-toughness materials was carried out by means of the unidirectional solidification method for eutectic composites such as ZrB_2–B_4C, $ZrO_2(Y_2O_3)$–NiO and $ZrO_2(Y_2O_3)$–Al_2O_3 systems.

Raw materials with eutectic compositions were blended in an alcohol slurry, pressed into rods, and sintered up to the theoretical densities. The sintered rods were machined into the dimensions of 7~10mm in diameter and 50mm in length.

Directional solidification was performed with a floating-zone furnace having halogen lamps in a cavity of dual ellipsoidal reflectors.

Both ZrB_2–B_4C and $ZrO_2(Y_2O_3)$–Al_2O_3 systems yielded aligned structures of ZrB_2 rods in B_4C matrix and, $ZrO_2(Y_2O_3)$ rods in Al_2O_3 matrix, respectively, whereas the $ZrO_2(Y_2O_3)$–NiO system gave lamellar structures of aligned planes.

Fracture toughness (K_{IC}) was measured by the indentation fracture (IF) method for polished sections parallel and perpendicular to the solidification direction. ZrB_2–B_4C system showed K_{IC} = 2.95 and 2.61MPa·$m^{1/2}$, respectively. These values can be recognized more than twice of fracture toughness of single crystal of matrix.

A fracture toughness of $ZrO_2(Y_2O_3)$–NiO systems depended on the mol% of Y_2O_3, and a remarkable anisotropy in K_{IC} was observed with respect to lamella directions. At the Y_2O_3 = 3mol%, K_{IC} (parallel) = 3.6MPa$m^{1/2}$ and K_{IC} (perpendicular) = 9.5MPa$m^{1/2}$ were obtained. It can be revealed that fracture toughness of these systems with aligned lamella structure was improved as much as three or nine times of constituent single crystals, depending on the lamella directions.

For the $ZrO_2(Y_2O_3)$–Al_2O_3 system anisotropy in fracture toughness was not appreciated with respect to solidification and transverse directions, resulting in K_{IC} = 5.0MPa$m^{1/2}$ for Y_2O_3 = 0mol%. Improvement of fracture toughness was achieved more than twice of single crystals of alumina matrix (K_{IC} = 2.1MPa$m^{1/2}$).

10. Surface Strengthening Technology With Coating

43070054U Tokyo FINE CERAMICS in English Mar 93 p 307

[English abstract of article by Osamu Sakai, Tomonori Takahashi, Hiroaki Sakai, Takao Soma, and Minoru Matsui, NGK Insulators Ltd.]

[Text] The surface coating for ceramics by CVD (chemical vapor deposition) has been developed to improve the oxidation resistance and to relax the surface contact stress of ceramics. The CVD-Si_3N_4 and CVD-SiC coating were applied to Si_3N_4 and SiC sintered body to improve the oxidation resistance. The CVD-Si_3N_4 and CVD-SiC coating conditions for Si_3N_4 sintered body were examined and established. The CVD-Si_3N_4 and CVD-SiC coated Si_3N_4 sintered body showed high oxidation resistance in static air compared to non-coated Si_3N_4 sintered body. This property was maintained even in the hot-gas corrosion test, and the strength of coated Si_3N_4 was almost maintained after the test where the noncoated Si_3N_4 showed a severe strength degradation. The CVD-TiN, TiC, TiB_2, and Al_2O_3 coating was applied to Si_3N_4 and SiC sintered body to relax the contact stress. TiN and TiC showed effect on relaxing the contact stress. The strength of CVD-coated materials were degraded by CVD coating. Si_3N_4-SiC composite coating was examined in order to improve the mechanical properties of the Si_3N_4 coating. Five-layer structure coating was obtained by controlling the atmosphere in the CVD reactor.

11. Nondestructive Inspection Technique

43070054V Tokyo FINE CERAMICS in English Mar 93 p 323

[English abstract of article by Yoshinori Tanimoto and Masami Tomizawa, Toshiba Corporation Fuchu Works; and Katsutoshi Nishida and Yutaka Abe, Toshiba Corporation Keihin Production Operations]

[Text] A prototype high-resolution X-ray CT scanner was fabricated by combining the micro-focus X-ray generator with a high-density X-ray detector array. The scanner's defect detection capability was evaluated using fine ceramics testpieces. It was proved that the instrument has an ability to detect artificial pinholes down to 38 μm diameter formed in a sintered silicon carbide (10mm outer diameter), and cracks of down to approximately 10 μm wide formed in a sintered silicon nitride (10.5mm outer diameter).

Nondestructive inspection techniques applicable to fine ceramics materials were studied on literatures. The studies showed that fine ceramics defects with sizes ranging from 10 to 30 μm in equivalent crack length were the target of detection. Because these sizes are very small-one-tenth to one-hundredth the sizes of defects in metallic materials, it is extremely difficult to detect them with the present nondestructive inspection techniques.

While there are many nondestructive inspection techniques studied so far, none of them seems to provide a complete solution for all kinds of defects in fine ceramics. Under specific conditions, however, the penetration testing (PT) is most effective for surface defects, the ultrasonic testing (UT) and scanning acoustic microscopy (SAM) for near-surface and internal defects, and the micro-focus X-ray radiography and micro-focus X-ray CT scanner for internal defects. The UT and SAM are difficult to apply to subjects with curved surfaces, however, since both utilize ultrasonic detection technique.

12. Proof Testing

12.1 Proof Testing Effects on Ceramic Components

43070054W Tokyo FINE CERAMICS in English Mar 93 p 350

[English abstract of article by Yoshihisa Sakaida, Research and Development Laboratory, Japan Fine Ceramics Center]

[Text] Some reliability-based designs are needed to apply the ceramic components for gas turbine engines. Proof testing is a very useful technique to assure the structural reliability of ceramic components. But some ceramics after proof testing have lower strength than the proof stress because of slow crack growth behavior. Therefore, it is quite important to estimate the minimum strength after proof testing.

In this study, a theoretical estimation of the minimum strength after proof testing was made for cyclic fatigue at elevated temperatures, then a statistical technique was proposed to estimate the actual minimum strength on a Weibull plot. Proof testings were also carried out on Si_3N_4 and SiC. The number of failure cycles was measured before and after proof testing. The results showed that the minimum strength after proof testing was evaluated on the Weibull statistical plot.

12.2 Proof-Testing Guide for Component of Ceramics Turbine

43070054X Tokyo FINE CERAMICS in English Mar 93 p 364

[English abstract of article by Akihiko Suzuki, Junichi Hamanaka, Koichro Tagasira, and Junsuke Okamura. Ishikawajima-Harima Heavy Industries Co., Ltd., Research Institute]

[Text] Proof testing is one of the most important technologies to assure the reliability of ceramic components. In this article, experimental and theoretical efforts are described to clarify the effects of various factors on the validity of proof testing. Factors such as proof testing temperature and cyclic fatigue damage are investigated experimentally by spin tests of circular plates and four-point bending tests of beam specimens with a rectangular cross section. To obtain a basis as to whether to omit a component in which flaws are detected by nondestructive testing and to establish the fracture criterion in the multiaxial stress state, combined mode I and II fracture toughness testing is conducted on knoop notched specimens. Also, an evaluation method based on the Weibull statistics and the slow-crack-growth theory is developed and effects of various factors on the validity of proof testing are investigated by using this method. On the basis of these investigations, a proof-testing guide for ceramic components has been newly developed and described here in a formal manner. It is the first trial in the world to develop a proof-testing guide for ceramic components, and the one proposed here is considered to be extended through experiences.

13. Analysis of Fracture Mechanics of Ceramics

13.1 Fracture Behavior Under Tensile and Combined Stresses

43070054Y Tokyo FINE CERAMICS in English Mar 93 p 380

[English abstract of article by Y. Nakasuji, H. Iwasaki, T. Makino, N. Yamada, S. Shimada, H. Sakai, H. Tsuruta, M. Masuda, and M. Matsui, NGK Insulators, Ltd.]

[Text] In order to clear the influence of variable mechanical factors on the strength properties of ceramic materials and develop the estimation, application, and design technique for a gas turbine component, various kinds of evaluations were carried out.

The strength of model specimens of a simulated gas turbine component was evaluated. Results agreed with predicted value based on the Weibull statistical theory using four-point-bending strength and tensile strength. Strength and fatigue behavior under multiaxial stresses were evaluated. The modified G-criterion is proposed for fracture criterion of silicon nitride (Si_3N_4) and silicon carbide (SiC). Fatigue behavior under multiaxial stresses has no difference in comparison with that under uniaxial stress. Fracture tests under contact stress were carried out by pin-on-disk test and ring-on-disk test. Surface damage by contact stress was influenced by friction, material, and temperature. Static fatigue tests of Si_3N_4 and SiC were carried out at elevated temperature. In Si_3N_4, there were two types of fracture regions. One is characterized by slow crack growth (SCG) and the other by creep deformation. In the SCG region, a power law type crack propagation equation is applicable to lifetime prediction. In the creep deformation region, the Larson-Miller parameter is applicable to lifetime prediction. In SiC, strength degradation was caused by slow crack growth. Cyclic fatigue tests of Si_3N_4 and SiC were carried out. In Si_3N_4, the failure diagram was constructed to show the effects of mean stress and stress amplitude on the fatigue strength under cyclic stress. The equation expressing the allowable stress under cyclic loading was proposed. In SiC, on-off behavior was shown at room temperature, but strength degradation was caused by slow crack growth at elevated temperature.

13.2 Stress Gradient Fracture

13.2.1 Static and Cyclic Fatigue

43070054Z Tokyo FINE CERAMICS in English Mar 93 p 428

[English abstract of article by Takashi Inamura, Seijiro Hayashi, Akihiko Suzuki, and Yasuhiro Shigegaki, Ishikawajima-Harima Heavy Industries Co., Ltd.]

[Text] The static and cyclic fatigue behavior of silicon nitride and silicon carbide was studied under four-point bending at room temperature and elevated temperature. The following studies were conducted; 1) the effect of stress gradient, frequency, stress ratio, temperature and variable stress amplitude on cyclic fatigue strength, 2) the effect of stress gradient and temperature on static fatigue strength, 3) the experimental and theoretical examination of the unified strength estimation method based on all data obtained in this study, and 4) the effect of atmosphere on static and cyclic fatigue strength of silicon nitride.

13.2.2 Bending Fracture Strength of Silicon Nitride Disks With Shoulder Fillet

43070054AA Tokyo FINE CERAMICS in English Mar 93 p 447

[English abstract of article by Seijiro Hayashi, Ishikawajima-Harima Heavy Industries Co., Ltd.]

[Text] Bending tests were performed on sintered silicon nitride disks with shoulder fillet at room temperature and 1000°C. Experimental fracture probability were compared with analytical predictions obtained by a structural reliability evaluation program, CCPRO. Results showed that: 1) the effective volume concept was applicable to biaxially loaded components, and 2) fracture criteria compared in this analysis gave little effect to fracture predictions.

13.2.3 In-Situ SEM Observation of Crack Propagation Behavior

43070054BB Tokyo FINE CERAMICS in English Mar 93 p 459

[English abstract of article by Masaki Kitagawa, Ishikawajima-Harima Heavy Industries Co., Ltd.]

[Text] Crack propagation behavior of Si_3N_4 and SiC was examined by scanning electron microscopy applicable to fatigue testing at high temperatures. Cyclic crack propagation in Si_3N_4 was found to be accompanied by certain types of deformation near the tip of the crack. All cases of crack propagation under cyclic tension and cyclic tension-compression load were similar in appearance. The enhancing effect of moisture on crack propagation under a static load was confirmed by in-situ observation. The effect of moisture under cyclic stress was not as under static stress. Crack propagation under low-stress level could be seen both in Si_3N_4 and SiC. Based on stress intensity analysis of an indentation cracked specimen, the cause of low-stress crack propagation was concluded to be a weak link fracture in the ceramics. Cracks propagated under decreased load when they did so under prior increasing stress.

13.2.4 Development of Precise Deformation Measurement System Based on the Concept of Moire Interferometry

43070054CC Tokyo FINE CERAMICS in English Mar 93 p 481

[English abstract of article by Seijiro Hayashi, Ishikawajima-Harima Heavy Industries Co., Ltd.]

[Text] A precise deformation measurement system based on the concept of moire interferometry was developed. The system consists of two parts: a rigid loading frame and an optical set-up for moire interferometry. An Argon ion laser with a coherent light of 514.5nm wavelength was used as a light source. The virtual reference grating method was employed to simplify the optical set-up. The accuracy of moire interferometry was verified by a single edge notched beam under three-point bending. The experimental results revealed that crack opening displacements (CODs) measured by moire interferometry agreed with calculated CODs by an empirical equation. It was found that the error was less than 2%. This system was intended to be used for analyzing the fracture process zone in ceramic composites in the next development stage.

13.3 Impact Fracture

4307005DD Tokyo FINE CERAMICS in English Mar 93 p 489

[English abstract of article by Tatsuya Yamada, Japan Fine Ceramics Center]

[Text] In the third period, the Japan Fine Ceramics Center (JFCC) has developed measuring methods of impact strength, two dynamic fracture toughness K_{Id} and K_{ID} of ceramics. K_{Id} means a dynamic stress intensity factor at the crack starting propagation under impact load. On the other hand, K_{ID} means a fracture toughness under the crack fast propagates.

In this work, a drop-weight type impact testing apparatus has been built up to measure the impact strength and K_{Id} of ceramics up to 1500°C. The strength of ceramics depended on the loading rate, but the K_{Id} depended on the loading rate. K_{Id} showed the tendency that is approximately proportionate to the dynamic stress intensity factor rate $dK_I(t)/dt$.

The pulsed holographic microscopy technique was applied to measure crack opening displacement (C.O.D.) and crack length of a fast propagating crack in ceramics. Using this technique, K_{ID} value can be estimated. In this period, we have built up a pulsed holographic microscopic measuring system for ceramics.

13.4 Fracture Behavior of Structural Ceramics in Corrosive Environments at High Temperature

43070054EE Tokyo FINE CERAMICS in English Mar 93 p 503

[English abstract of article by Takuya Kondo and Koichi Kojima, Toyota Motor Corporation]

[Text] Fracture behavior was investigated for structural ceramics such as Si_3N_4 and SiC in corrosive environments at high temperature. Thermal cycle and constant temperature oxidation tests were performed up to 1400°C in air. Flexural strength tests were made under three loading rate conditions at 1250°C in various atmospheres using pre-crack specimens by knoop indentation. Corrosion tests were performed under various stress conditions using specimens coated with molten salts at 1000°C in air. The following results were obtained by analysis of chemical reaction and material strength.

(1) Strength of Si_3N_4 reduced at room temperature after oxidation because of crack formation in the oxidized layer. Strength at high temperature after oxidation did not change, because the crack disappeared by melting of the oxidized layer.

(2) Strength of Si_3N_4 did not reduce after thermal cycle oxidation test beyond 20Hr in accumulated exposure time. The surface morphology of Si_3N_4 did not change with accumulated exposure time.

(3) Strength Of Si_3N_4 with pre-crack increased under a low-loading rate condition because of crack healing or shortening by oxidation in oxidizing atmospheres.

(4) Molten salts of sodium corroded Si_3N_4 at 1000°C in air. The major mode of corrosion attack is dissolution of the grain boundary phase, and the formation of wide pits results in strength reduction.

(5) Applied stress affected the morphology of bubbles in the corroded layer by molten salts. One model is proposed for the bubble formation in the corroded layer under tensile stress and compressive stress.

13.5 Corrosion Under High-Temperature Atmosphere

43070054FF Tokyo FINE CERAMICS in English Mar 93 p 521

[English abstract of article by Yoshiro Noda, Takashi Okamura, Toru Shimamori, and Masakazu Watanabe, R&D Center, NGK Spark Plug Co., Ltd.]

[Text] Corrosion behavior of Si_3N_4 and SiC ceramics was investigated. The corrosion tests were performed under several atmospheres (O_2, air, combustion gas of C_4H_{10}, CO_2, and N_2) and by loading of corrosive materials (Na_2CO_3, Fe_2O_3, $CaCO_3$, and coal ash). Weight gain after oxidation was almost equal under every atmosphere except Ni. The flexural strength after corrosion tests decreased. The metal elements of sintering additive oxides depleted near the interface between oxidized layer and silicon nitride and migrated into the oxidized layer.

Next, influence of corrosive materials on the corrosion resistance of Si3N4 and SiC ceramics was investigated. Loading of corrosive materials enhanced corrosion and the corrosion resistance of SiC and Sc_2O_3 doped Si_3N_4 ceramics were better than that of Y_2O_3-Al_2O_3 doped Si_3N_4 ceramics.

The corrosion level for nonoxide ceramics used under a corrosive environment under which the gas turbine was operated can be estimated by the corrosion test condition as below.

(1) Gas corrosion
Atmosphere: air temperature: 1400°C
Holding time: 100 hours

(2) Coal ash corrosion
Loading rate: 1.0-2.0 mg/cm^3
Atmosphere: Air
Temperature: 1400°C
Holding time: 10 hours

13.6 Thermal Fatigue Behavior

43070054GG Tokyo FINE CERAMICS in English Mar 93 p 533

[English abstract of article by Nobuo Ayuzawa and Masamichi Takai, New Materials Research Center, Shinagawa Refractories Co., Ltd.]

[Text] The objective of this study is to investigate the thermal fatigue behavior of the silicon nitride and silicon carbide in relation to some properties after thermal cycling and heat treatments in some gaseous environments. For this objective, JIS standardized and hollow cylinder shaped specimens with and/or without notch were examined under thermal cyclic and heat treatments.

The results obtained are summarized as follows.

1. Silicon nitride and silicon carbide were heated in gaseous environments such as H_2, CO, CO_2. These materials are strongly affected on the weight, phase components, microstructure and strength especially by reduction gases such as H_2 and CO.

2. Thermal cycling of hollow cylinder shaped specimens with notch of silicon nitride were tested. Stress concentration occurred during thermal cycling and maximum thermal stress is about 1100MPa at the specimen having most sharp notch. Crack propagation were observed in the direction of diameter by thermal cycling that is caused by thermal stress concentration.

3. Thermal cycling of the specimens after gas exposure were tested in a nitrogen atmosphere at 1300°C for 10^3 cycles. Strength degradation was not observed during thermal cycling. It is considered that the change of the microstructure of the surface during gas exposure affected the thermal conditions at thermal cycling.

14. Design Guide for Ceramic Components

43070054HH Tokyo FINE CERAMICS in English Mar 93 p 549

[English abstract of article by Akihiko Suzuki and Junichi Hamanaka, Ishikawajima-Harima Heavy Industries Co., Ltd.]

[Text] To apply a ceramic material to structural components, it is necessary to develop the evaluation method for the strength of ceramic components and to develop a design guide for ceramic components based on the above-mentioned method.

In the present article, a design guide for ceramic components is described. The design guide is developed as a unification of a design guide preventing fast fracture of ceramic components and one preventing time-dependent fracture which were developed during the second stage of this project. An extended version of the above-mentioned design guide is also developed as a design guide for ceramic gas turbine components including an elaborate method of estimating the Weibull modulus, additional values of design factors, formulas for environmental effects and FOD. The consistency with the proof testing guide also developed in this project.

As activities of developing evaluation methods for the strength of ceramic components, two computer programs are developed and described here. They are a simulation program of the impact damage of ceramic components and a reliability analysis program which considers the effect of the inelastic deformation of ceramic components. These kinds of programs do not exist very widely in the ceramic technology.

Chapter 2. Integration of Technology R&D

1. Objectives, Outline of Integrated Technology R&D

94FE0398B Tokyo FINE CERAMICS in Japanese Mar 93 pp 569-570

[Text] During the last two years of the project, which was devoted to integrated technology R&D, attempts were made to use the monolithic materials to produce stator and rotor models equipped with various elements for ceramic gas turbine components for coal gasification, and carry out integrated evaluation tests on these models, while efforts were made to achieve the target values for the toughness-reinforcing materials and to clarify their toughness reinforcement mechanisms.

The monolithic materials included one type of silicon nitride (sintered in two stages, and highly corrosion resistant) and two types of silicon carbide (one sintered with an alumina-based sintering aid, and the other sintered with a boron-carbon-based sintering aid). Except for metallic silicon, the raw material powders that had been developed in this project were used to make these materials, from which stator models were produced by different molding processes based on previous development results. In contrast, a rotor model was injection-molded from another type (high strength) of silicon nitride. Many previous research accomplishments were also adopted in HIP-involving sintering conditions. The models arc shown in Figure 1. In order to verify performances against heat shock and high-temperature, high-speed rotation, the models were tested with the device shown in Figure 2 with combustion gas to maintain the stator and the rotor at 1,400°C and 1,250°C, respectively. However, prior to these tests, the sintered models had been forwarded to the respective corporations in charge which had machined to finish the models, bonded the rotor model with the rotation shaft, reinforced the model's surface with coating, carried out nondestructive inspection and guarantee tests.

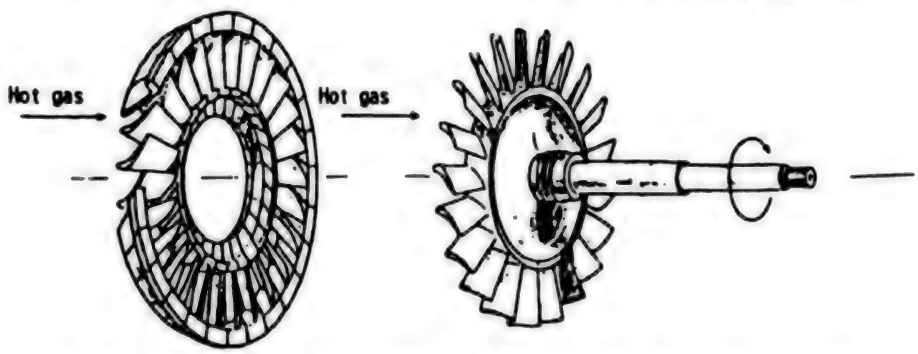

Figure 1. Models for Integrated Technology Verification Tests (Left: Stator; Right: Rotor)

Furthermore, in order to confirm whether the target values were achieved or not, the respective corporations in charge as well as the national research institutes and private corporations in charge of evaluation tested cut-out testpieces from the models and sintered materials for strength, reliability (Weibull constant), fracture toughness, delayed fracture strength (10,000 hours), stationary and dynamic corrosion and heat fatigue resistance.

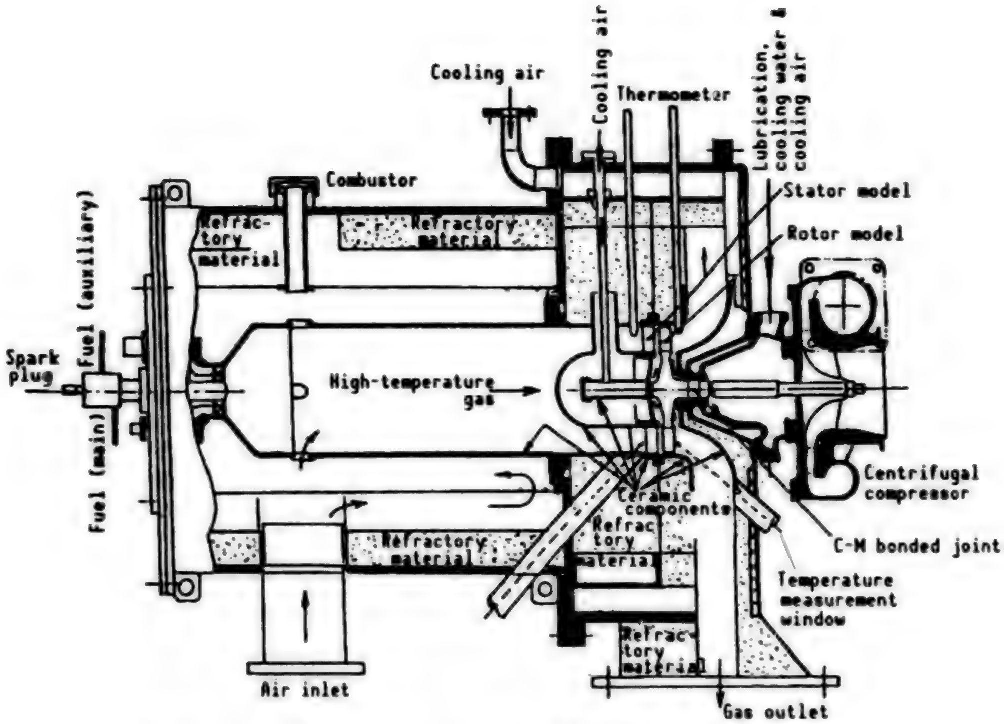

Figure 2. Main Part of Verification Test Device

Studies concerning the toughness reinforcing materials were continued along the separately planned paths, and some of the materials were found to have achieved target values. The plan was altered for the study concerning boron-containing silicon carbide in an attempt to develop a particle-dispersed high-toughness material: i.e., the method of theoretically calculating this material's internal stress caused by the property differences between the dispersed particles and the matrix, and a high-toughness material was prepared based on this method.

Although a few, there were some newly discovered pieces of fundamental knowledge acquired from the above-described mainstream R&D activities. One example was the fact that the high-temperature strength of silicon nitride depended on the halogen content of the raw material powders.

2. Element Technology for Turbine Components

2.1 Molding and Sintering of Stator Model

2.1.1 Silicon Nitride Material

43070054II Tokyo FINE CERAMICS in English Mar 93 p 571

[English abstract of article by Yasuhiro Takagi, Yoshio Hayashi, Yoshiro Noda, Toru Shimamori, Masakazu Watanabe, and Yasushi Matsuo, R&D Center, NGK Spark Plug Co., Ltd.]

[Text] Post-sintered silicon nitride doped with Sc_2O_3 as a sintering additive was applied to stator model material used at 1400°C for ceramic gas turbine. Post-sintering is one of the sintering processes in which reaction-bonded silicon nitride was sintered to be densified.

The green bodies of a stator model was fabricated by slip-casting with silicon slurry. The range of viscosity which was adequate to slip-casting was 100~200cP. In this range, the pores in the green body were not detected by the observation of X-ray photography. The green bodies of a stator model were nitrided at the maximum temperature of 1450°C in nitrogen plus hydrogen gas flow. Subsequently, post-sintering was performed by sinter-HIPing. HIPing was at 1800°C for 2 hours under the nitrogen pressure of 196MPa.

The density of the HIPed stator model reached to almost full density. The stator model was sintered homogeneously by lowering the heating rate above the temperature in which shrinkage of the model occurred. Next, mechanical properties of cut-off testpieces from the HIPed stator model were evaluated. The four-point bending strength corresponding to 20% of failure probability was 408MPa and the Weibull modulus (m) was 21.7. By changing four-point bending effective volume into stator model effective volume, the fracture strength (σ, 20%) was 457MPa. Both values satisfied the target values (σ, 20% $\geq$ 400MPa and m $\geq$ 20, respectively). Fracture toughness measured by the single-edge precracked beam (SEPB) method was 5.0MPam$^{1/2}$, which attained to the target value ($\geq$3MPam$^{1/2}$).

2.1.2 Development of Integrated Stator-Nozzle Models by Injection Molding of Silicon Carbide With the Addition of Alumina

43070054JJ Tokyo FINE CERAMICS in English Mar 93 p 586

[English abstract of article by Takashi Kanno and Nobuhiro Shinohara, Asahi Glass Co., Ltd., Research Center]

[Text] The integrated stator-nozzle model for ceramic gas-turbine has been developed with monolithic silicon carbides through "injection molding" plus "pressureless sintering" plus "HIPing" processes by use of β-SiC powders with sintering aid of 5wt% alumina. The 52.5vol% of silicon carbide powders with alumina were compounded with binder (polyethylene and polystyrene) by addition of a plasticizer (octyl palmitate) and lubricant (stearic acid and stearyl alcohol) to achieve uniform dispersion of powders in polymer melts.

The dimensional accuracies were evaluated for as-molded, pressureless sintered, and HIPed segments of the stator model with respect to the coefficient of variation among the separate segments of the stator models. The coefficient of variation was controlled to less than 0.72%. Average linear-shrinkage of 20.35% resulted with a standard deviation of 0.69% and the coefficient of variation of 3.39% for the HIP'ed stator models of the bulk density of 96.42%TD.

The mechanical properties of each segment of the stator models were evaluated with testpieces cut from outer shrouds of the separate stator models and eventually the performance of the stator-nozzle models was confirmed by integrated evaluations of repeated thermal shock tests at IHI.

(1) Flexural strength: σ_{3P} = 595MPa (1400°C) with Weibull modulus: m = 20 was obtained by three-point bending tests. A minimum guaranteed strength, defined in this project as fast-fracture strength of failure probability, of 20% estimated for effective volume of the stator model (VE = 0.25mm^3), was evaluated as σT (20%) = 581MPa (target value ≥ 400MPa at 1400°C).

(2) Creep rupture strength: σ_{4P} ≥ 250MPa (1400°C-10,000h) was obtained by four-point bending test at 1,000h (target value ≥ 250MPa at 1400°C for 10,000h).

(3) Fracture toughness: K_{IC} = 5.7MPam$^{1/2}$ was achieved by the single-edge precracked beam (SEPB) method (target value ≥ 3MPam$^{1/2}$).

(4) The performance of the stator-nozzle models was confirmed by integrated thermal shock tests at IHI.

2.2 Development of Silicon Nitride Integration Period Model

4307005KK Tokyo FINE CERAMICS in English Mar 93 p 602

[English abstract of article by K. Nishida, T. Kameda, M. Asayama, T. Suto, A. Tsuge, Y. Goto, and T. Fukazawa, Toshiba Corporation; and T. Kanda, T. Tatsuno, and T. Takebe, Kobe Steel, Ltd.]

[Text] In the integration period of '91-'92, the integration of materials and process technologies, developed in previous research phases, was attempted. As the model for this integration, a rotor with 20 blades was introduced. The following research and development items were studied on silicon nitride material base.

(1) Development of material with higher strength and creep resistance at 1250°C using raw powder developed in this project as the starting material.

(2) Development of a fabrication process for the integration period model.

(3) Evaluation of high-temperature mechanical properties using a test bar cut from the model.

Target qualities and the fabrication process are the same as the previous phase. Developed material showed possibility to withstand 10,000 hrs under 1250°C x 250MPa creep condition. The strength of 617MPa (at blade neck, and at 20% failure probability), a Weibull modulus of 36, and a fracture toughness of 7.0MPam$^{1/2}$ were obtained by test bar cut from the model. These data satisfied target values for this period.

2.3 Development of High-Efficiency Machining for Ceramics

43070054LL Tokyo FINE CERAMICS in English Mar 93 p 615

[English abstract of article by Masahiro Okamoto, Yasuo Niino, and Naoto Ono, Toyoda Machine Works, Ltd.]

[Text] Machinability is different between silicon carbide with an additive of B_4C and C and silicon carbide with an additive of Al_2O_3. Using a strong grinding wheel, it can be realized to grind the silicon carbide with an additive of Al_2O_3 at the grinding efficiency of 100mm^3/mm·s and with a grinding ratio of 6000. It is important to minimize the impact during the grinding of silicon carbide with the additive of B_4C and C, because its K_{IC} is small, and therefore, friable.

In high-efficiency grinding of various kinds of ceramics, there can be recognized a correlation between the grinding resistance and bending strength at a high temperature.

2.4 Joining Technology

2.4.1 Joining of Bladed Disk Model

43070054MM Tokyo FINE CERAMICS in English Mar 93 p 625

[English abstract of article by Hisao Takeuchi and Akira Yamakawa, Itami Research Laboratories, Sumitomo Electric Industries, Ltd.]

[Text] We investigated joining of the bladed disk model made of silicon nitride. On the basis of multilayer metallizing (Ti-Ni-Au) by the ion-plating method followed by brazing developed in the third period of the project, a joining process applicable to the bladed disk model and the metal shaft was investigated.

Differences in joining structure from before were using shrink fitting together with brazing and an addition of electron-beam welding process. That was for reduction of stress and heat shock to the joining part and this is for softening prevention of metal shaft (SNCM-steel) and for an easy nondestructive test of joining the interface. We attached importance to confidence of joining process. The ultrasonic image analysis to joining interface and the proof test by giving flexural stress at last stage were performed.

We think, these investigations and some preliminary experiments have established the joining process of the bladed disk model. According to this process joining of the model and the metal shaft was performed for demonstration of the ceramics turbine.

2.4.2 Model of Silicon Carbide Nozzle for Ceramic Gas Turbine

43070054NN Tokyo FINE CERAMICS in English Mar 93 p 642

[English abstract of article by K. Koga, S. Kohsaka, S. Nagano, M. Terazono, and S. Tateno, Central Research Laboratory, Kyocera Corporation]

[Text] A silicon carbide nozzle was prepared by using a pure, fine powder and joining technology developed in the FC-Project. A vane and shrouds of green compact were joined with a silicon carbide powder paste and then sintered together. The nozzle was successfully tested in gas turbine test equipment and confirmed its thermal resistance.

The cyclic cold isostatic pressing (CIP) method was applied to improve material properties and reliability. The cyclic CIP can increase the green compact density up to 75% of theoretical density. The cyclic CIP method was effective to densify uniformly the thick green compact. The higher the green density the average size of void becomes smaller. [Figures 6, 7, 8 and 9 follow.]

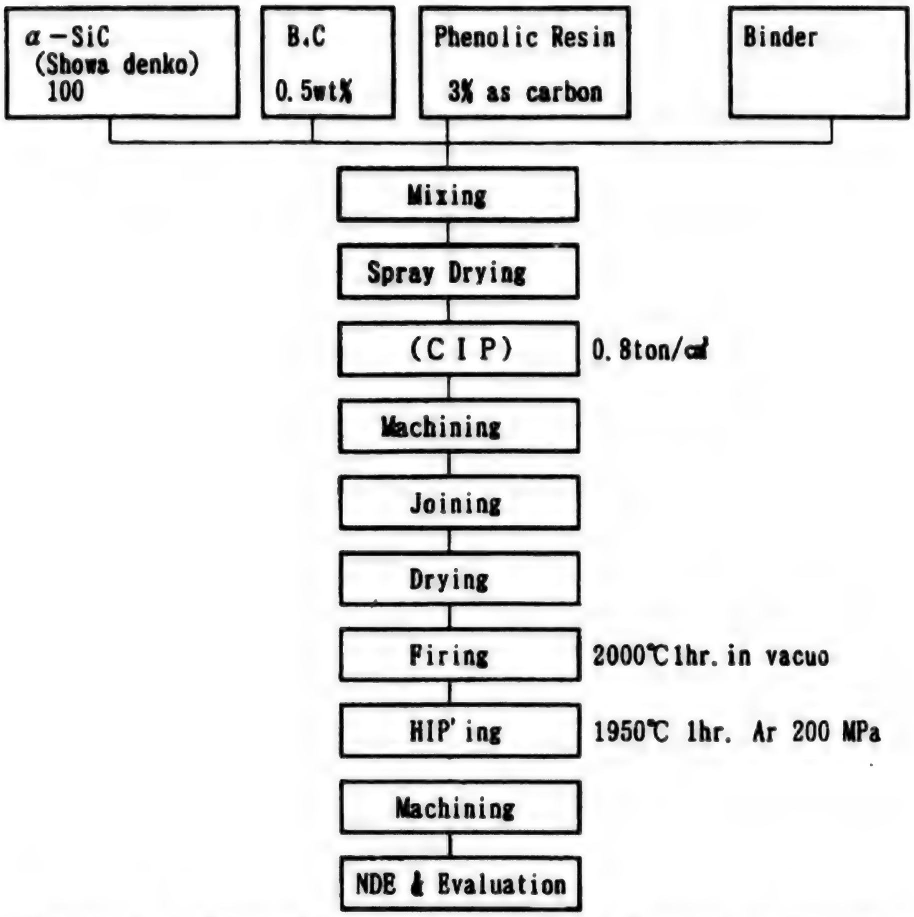

Figure 6. Scheme of the Preparation of Nozzle by Joining

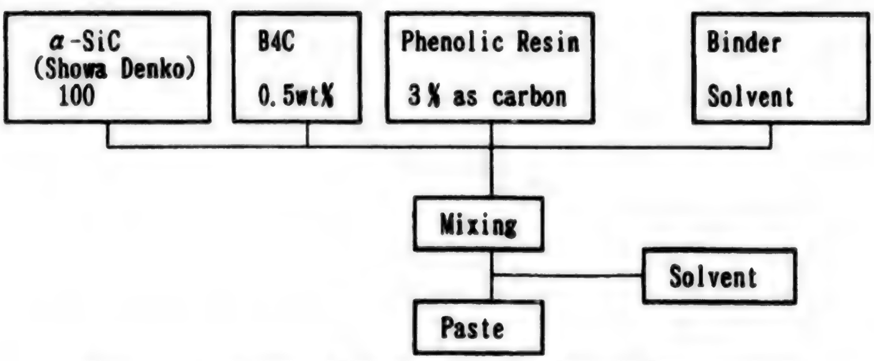

Figure 7. Scheme of the Joining Paste Preparation

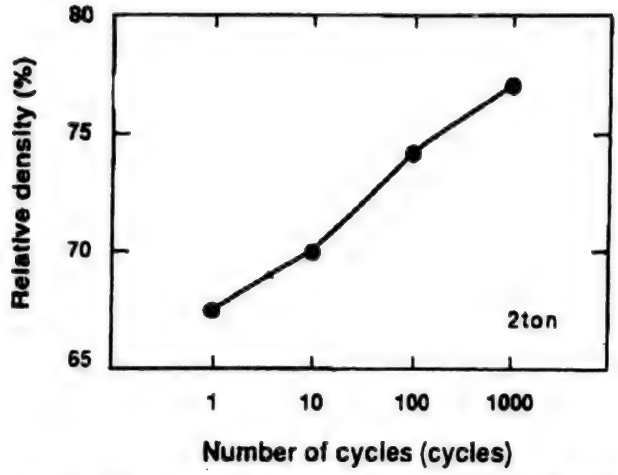

Figure 8. Density Change as a Function of Number of Pressure Cycles (Pmax: 196 MPa)

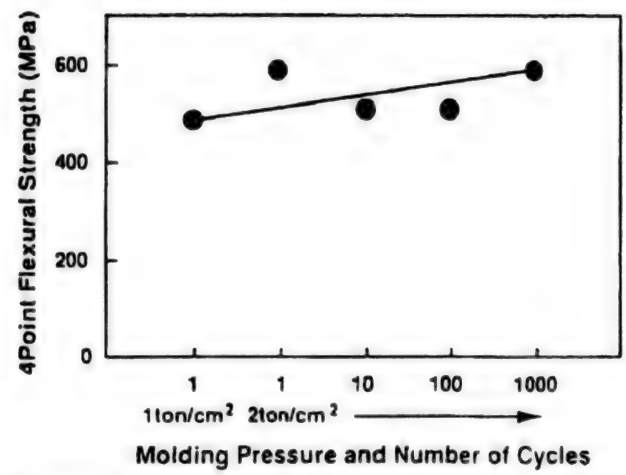

Figure 9. Flexural Strength of Cyclic CIP'ed Test Bars as a Function of Number of Cycles

2.5 Surface Strengthening Technology

4307005400 Tokyo FINE CERAMICS in English Mar 93 p 656

[English abstract of article by Osamu Sakai, Tomonori Takahashi, Takao Soma, and Minoru Matsui, NGK Insulators Ltd.]

[Text] In the third phase of the fine ceramics project, the CVD-Si_3N_4 and CVD-SIC coated Si_3N_4 sintered body showed high oxidation resistance compared to the noncoated Si_3N_4 sintered body. In the fourth phase, the CVD-Si_3N_4 and CVD-SiC coating has been developed to improve the oxidation resistance of the sintered Si_3N_4 rotor model and sintered SiC stator model which were developed during this project. The CVD-Si_3N_4 and CVD-SiC coating was applied to the Si_3N_4 and SiC sintered body, respectively. The CVD-Si_3N_4 and CVD-SiC coating condition for large-size complex substrate was examined to obtain the homogeneous coating on the models. The CVD-Si_3N_4 and CVD-SiC homogeneous coating was obtained by control of introducing gases around the substrate. The CVD coated Si_3N_4 rotor and SiC stator model were subjected to the rig test. The oxidation resistance and mechanical properties of CVD-Si_3N_4 and CVD-SiC coated Si_3N_4 and SiC sintered body were evaluated. The CVD coated Si_3N_4 and SiC sintered body showed high oxidation resistance compared to the noncoated sintered body. However the strength of the CVD-Si_3N_4 coated Si_3N_4 sintered body was degraded by CVD coating. The reason for the degradation was due to the low strength of Si_3N_4 coating. The SiC dispersed Si_3N_4 composite coating was examined in order to improve the mechanical properties of the Si_3N_4 coating. However the composite coating was not obtained.

2.6 Nondestructive Inspection Technique

43070054PP Tokyo FINE CERAMICS in English Mar 93 p 673

[English abstract of article by Yoshinori Tanimoto and Masami Tomizawa, Toshiba Corporation Fuchu Works; and Katsutoshi Nishida and Yutaka Abe, Toshiba Corporation Keihin Product Operations]

[Text] In order to explore nondestructive testing methods applicable to ceramics components, the secondary and overall wing models of rotors and stators were adopted. The results of the studies were compiled into a manual for nondestructive testing for each model.

The nondestructive testing methods best suited for the objective models with different figures, sizes, and materials were chosen according to the results of past studies. For the second wing models, penetration testing (PT) was chosen for surface defect inspection, ultrasonic testing (UT) for near-surface and internal defect inspection, and micro-focus X-ray radiography and X-ray CT scanner for internal defect inspection. Three out of the four testing methods —except the UT method—were selected for the overall wing models most of which consisted of curved surfaces. Those testing methods were actually applied to nondestructive inspection to optimize the inspection conditions for each part of the models.

Surface defects were probed with PT and visual inspection. Internal defects were first photographed with the micro-focus X-ray radiography. Surface defects included in the films were then separated from internal defects; also with PT and visual inspection. This approach proved to be almost feasible for field testing.

2.7 Proof Testing

2.7.1 Proof Testing for Ceramic Gas Turbine Components

43070054QQ Tokyo FINE CERAMICS in English Mar 93 p 691

[English abstract of article by Yoshihisa Sakaida, Research and Development Laboratory, Japan Fine Ceramics Center]

[Text] An application of ceramic components to the gas turbine engine must take into account the mechanical reliability assurance that components will not fail under service conditions. Therefore, the successful practical use of a ceramic gas turbine requires the development and enforcement of proof testing as a method of eliminating the components, including defects.

In this study, the strength degradation during proof testing was estimated using fracture mechanics in case the proof stress mode was different from the actual state. A proof-testing method for ceramic turbine blades was developed by improving the proof-testing techniques that were obtained in the previous period III of this project. Proof testings were carried out on each stator blade by thermal shock stress. The results showed that the strength distribution of stator blades after proof testing was truncated, and the reliability of turbine blade assembly could be assured to the thermal shock in an emergency.

2.7.2 General Evaluation of Proof-Testing Guide

43070054RR Tokyo FINE CERAMICS in English Mar 93 p 711

[English abstract of article by Akihiko Suzuki, Seijiro Hayashi, Junsuke Okamura, and Koichiro Tagashira, Ishikawajima-Harima Heavy Industries Co., Ltd., Research Institute]

[Text] A proof-testing guide for ceramic components was proposed and modified up to the third development stage. The modification was made by including results of theoretical and experimental examinations concerning various factors related to proof testing. Although the guide is rational and systematic, it has been verified only by a few simple experimental results. The applicability of the guide to cases which involve complexity of stress and temperature distribution or time dependent stress and temperature distribution has not yet been clarified. In the generalized evaluating stage, an experimental investigation using beam specimens with shoulder fillet was carried out to study the effect of loading modes on proof testing. Moreover, a few theoretical examinations were given to confirm the validity of the guide. Finally, a proof test for generalized testing models was conducted in accordance with the proof testing guide. [Figures 18, 19, 20 and 21 follow.]

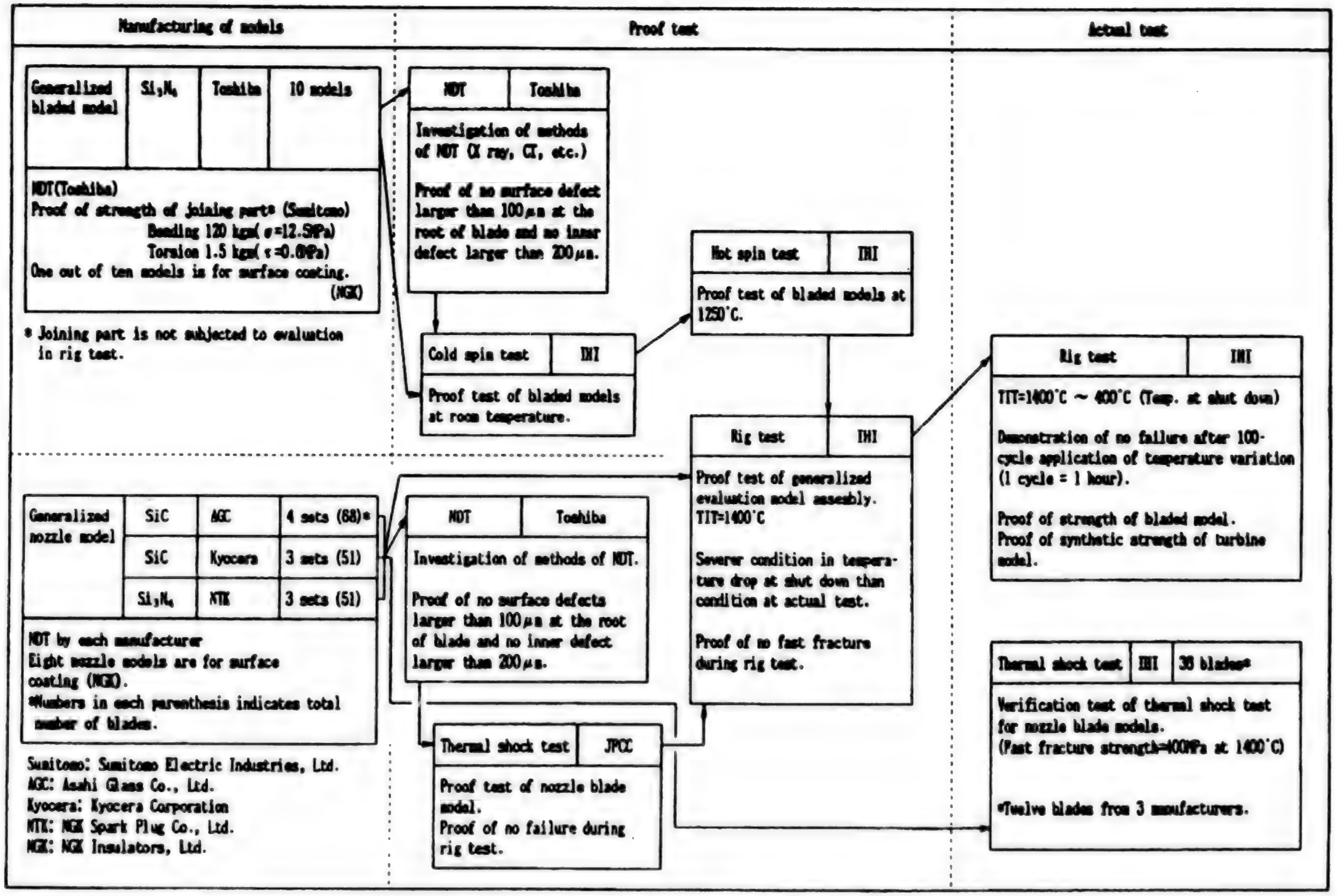

Fig. 18 Plan for generalized evaluation test

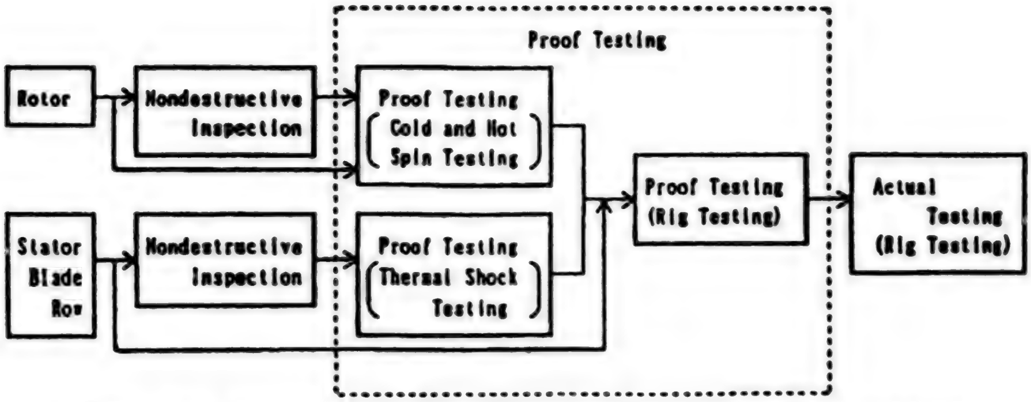

Figure 19. Flowchart of Prooftesting Process in Generalized Evaluation Test

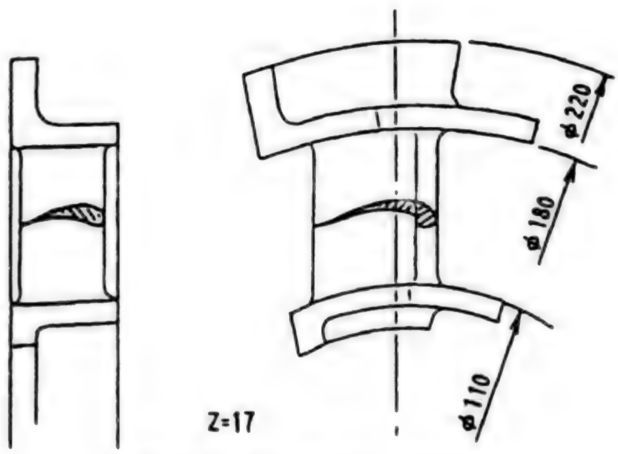

Figure 20. Nozzle Model

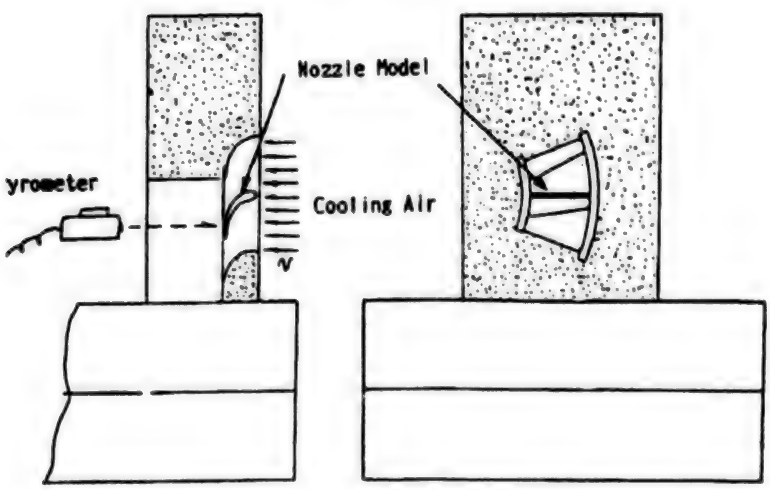

Figure 21. Thermal Shock Test for Nozzle Model

2.8 Generalized Evaluation Test

43070055S Tokyo FINE CERAMICS in English Mar 93 p 738

[English abstract of article by Junsuke Okamura, Koichiro Tagashira, Kouichi Katohno, and Masaru Mizuhashi, Ishikawajima-Harima Heavy Industries Co., Ltd., Research Institute]

[Text] Structural ceramic components have been fabricated and evaluated for strength at high temperature to apply a hot section of a gas turbine. Usually turbine blades encounter various modes of loading, such as centrifugal, thermal, aerodynamic, vibratory load, and so on. Therefore, a turbine blade should be designed considering the various operating conditions. The test model is a bladed Si_3N_4 disk made by injection molding and after that HIP treatment is done. The model disk has 20 blades that are two-dimensional along the blade height and joined by a metal shaft. The effective volume of model amounts to $126mm^3$. The maximum stress arises at the blade root. The value of design stress at this section is determined by the design guide that has been studied in this section. The test apparatus can evaluate the rotating strength of the model assembled with nozzles over 50,000 rpm and TIT of 1400°C. Before hot spin testing, bladed disks were truncated by cold spin testing. After that, the strength of the bladed disks was experimentally evaluated by hot spin testing at TIT of 1400°C. It was revealed that the rotating strength of the test model at TIT of 1400°C was more than 307MPa at the fast-fracture mode.

2.9 Materials Evaluation

2.9.1 High-Temperature Strength/Toughness

2.9.1.1 Static and Cyclic Fatigue

43070054TT Tokyo FINE CERAMICS in English Mar 93 p 753

[English abstract of article by Takashi Inamura, Akihiko Suzuki, Seijiro Hayashi, and Yasuhiro Shigegaki, Ishikawajima-Harima Heavy Industries Co., Ltd.]

[Text] Static and cyclic fatigue behavior of the materials developed in this project were studied to provide the data for evaluating the strength of model components used in the generalized evaluation test. Fatigue tests of silicon carbide developed in this project and commercially available silicon nitride were also conducted under inert gas atmosphere along with the analysis of the effect of gas atmosphere on the fatigue property.

The applicability of the unified strength estimation method was tested under various conditions. It was found that the unified strength estimation method can be applied to estimate the effect of temperature on fast fracture, static fatigue, and cyclic fatigue properties.

2.9.1.2 Fracture Strength of Rotor Blade Models and Disks With Shoulder Fillet

43070054UU Tokyo FINE CERAMICS in English Mar 93 p 776

[English abstract of article by Takashi Inamura, Seijiro Hayashi, Akihiko Suzuki, Hidenari Baba, and Shunji Kasa, Ishikawajima-Harima Heavy Industries Co., Ltd.]

[Text] A fracture test was conducted on silicon nitride rotor blade model specimens to examine the applicability of the strength evaluation method for ceramics. The method was based on the Weibull statistical theory and linear fracture mechanics. Specimens were loaded to fracture in combined bending and torsion. The fracture stress conditions were examined in the multiaxial and distributed stress state compared to the expected strength by the evaluation method. It was revealed that the strength evaluation method is applicable to ceramic components.

2.9.1.3 In-Situ SEM Observation of Crack Propagation Behavior

43070054VV Tokyo FINE CERAMICS in English Mar 93 p 786

[English abstract of article by Isamu Nonaka, Ishikawajima-Harima Heavy Industries Co., Ltd.]

[Text] Crack propagation of Si_3N_4-SiCw under dynamic fatigue loading and cyclic fatigue loading were examined by scanning electron microscopy (SEM) applicable to fatigue testing at high temperatures. The following results were obtained:

(1) Stable crack propagation from the indentation crack was observed on more than half of the fracture load under dynamic loading.

(2) Relationship between load and crack growth amount was not dependent on the loading rate under dynamic loading.

(3) The deflection and pinning of the crack by the SiC whisker were observed under dynamic loading and cyclic loading.

As a result the toughening mechanism of the composites was confirmed.

2.9.1.4 Analysis of Fracture Process Zone in Ceramic Composite by Moire Interferometry

43070054WW Tokyo FINE CERAMICS in English Mar 93 p 796

[English abstract of article by Seijiro Hayashi, Ishikawajima-Harima Heavy Industries Co., Ltd.]

[Text] The fracture process zone in Si_3N_4/SiCw ceramic composite was analyzed by a hybrid experimental-numerical procedure employing moire interferometry. A chevron-notched, wedge-loaded double cantilever beam specimen was used to obtain a stable crack growth. The crack tip obtained from the moire pattern was located 0.3 mm behind the true crack tip. A possible explanation for the result was that the crack opening displacement ahead of the moire-specified-crack tip was less than the sensitivity of moire interferometry. Fractographic study showed that toughening of this material was not provided by pullouts. However, a combination of debonding and bridging was a possible toughening mechanism. The relation of crack closure stress versus crack opening displacement in the fracture process zone was obtained. It was also found that fracture probability of a component was joint fracture probability of the fracture process zone and the rest of the component outside the fracture process zone. Further studies of relation between R-curve behavior and Weibull modulus are required for improving the design guide.

2.9.2 Delayed Fracture Strength

43070054XX Tokyo FINE CERAMICS in English Mar 93 p 807

[English abstract of article by Tatsuki Ohji and Yukihiko Yamauchi, Government Industrial Research Institute, Nagoya]

[Text] This study was aimed at investigating long-term (up to 10,000 hours) tensile creep and creep rupture behavior primarily of the materials developed in this R&D project. The test temperature was designated as 1250°C for the rotor materials, and 1400°C for the stator materials.

First, in order to obtain the fundamental information of tensile creep of common ceramics, commercially available hot-pressed silicon nitride had been tested at 1200°C through 1350°C. A stable, steady state was observed under low applied stresses at 1200°C. Accelerated creep regimes which were absent below 1300°C, were identified above that temperature. The appearance of accelerated creep at the higher temperatures is attributable to formation of microcracks throughout a specimen. The primary creep mechanism was considered cavitation enhanced creep. Specimen lifetimes followed the Monkman-Grant relationship except for fractures with large accelerated creep regimes.

Five grades of the developed materials have been subject to long-term creep testing: silicon nitrides doped with Sc_2O_3, doped with Yb_2O_3, and doped with Y_2O_3, and silicon carbides doped with Al_2O_3 and doped with B and C. Silicon nitride doped with Sc_2O_3 was tested at 1400°C, and showed similar creep behavior to those of the above commercially available one at 1200°C under a similar stress range; long steady state creep regimes were obtained and the Monkman-Grant relationship was well applied. Cavitation enhanced creep was predominant, partly contributed by solution-reprecipitation. A lifetime of 10,000 hours has been verified under the stress of 50MPa. Silicon nitride doped with Yb_2O_3 showed only transient creep until failures, which were controlled by a slow crack growth. The failure occurred in some 3,000 hours at 200MPa. Very excellent creep resistance has been observed in yttria-doped silicon nitride, recently developed material, though 1,000 hours has passed so far.

A lifetime of some 8,000 hours was verified at 1400°C, 200MPa for alumina-doped silicon carbide. The creep rate decreased with time, down to $6x10^{-12}$/sec in some thousand hours. The failure occurred by a slow crack growth. It was suggested that a diffusive crack propagation model was applicable, and a threshold (safety) applied stress was present. No detectable creep deformation was obtained for silicon carbide doped with boron and carbon at 1400°C, 200MPa, preceded by a very small strain increase in the first 3,000 hours. The test was interrupted after 10,048 hours.

2.9.3 Erosion Properties of Ceramics

43070054YY Tokyo FINE CERAMICS in English Mar 93 p 831

[English abstract of article by Mikio Iwasa and Makoto Kinoshita, Government Industrial Research Institute, Osaka]

[Text] The degradation of solid surface by high velocity particle impingement is called erosion. The accumulation of surface microcracks introduced by particle collisions will cause surface removal and reduction in mechanical strength. We adopted the micro-blaster method to measure the erosion, because the small sample size is enough and a wide range of experimental conditions can be used.

The erosion volume, which was obtained by numerical approximation of wear scar cross section to the Guassian curve, was in good agreement with weight loss measurement. The erosion resistance was on the order of alumina, silicon nitride, toughened zirconia, silicon carbide, mullite, magnesia, and fused silica was worst. The strength degradation, measured by the bending method before and after erosion test, was in positive correlation with erosion volume.

The erosion properties of the monolithic C-band materials developed through this project were also measured. The erosion volume of silicon nitrides was greater than that of silicon carbides, but they retained more strength after erosion.

2.9.4 Fracture Behavior of Structural Ceramics in Corrosive Environments at High Temperature

43070054ZZ Tokyo FINE CERAMICS in English Mar 93 p 840

[English abstract of article by Takuya Kondo and Koichi Kojima, Toyota Motor Corporation]

[Text] Fracture behavior was investigated on developed Si_3N_4 (SN-A, SN-B), developed SiC (SC-A, SC-B), and ceramics on the market (Si_3N_4 (SSN), SiC (SSC)) in corrosive environments at high temperature. Exposure tests were performed using specimens coated with coal ashes and molten salts at 1,000°C, 1,250°C, and 1,400°C in air. Flexural strength tests after exposure were performed at room temperature and up to 1,400°C in air. The following results were obtained by analysis of chemical reaction and material strength.

(1) The corrosion resistance of developed ceramics were better than that of ceramics on the market. SN-A coated with coal ashes did not corrode up to 1,250°C in air for 200h. SN-B, SC-A, and SC-B coated with coal ashes did not corrode up to 1,400°C in air for 200h, and the high-temperature strength of these ceramics did not decrease after exposure.

(2) The corrosion of SSN coated with FeO occurred at 1,250°C, 1,400°C in air. Room-temperature strengths of corroded SSN by coal ashes reduced because of crack formation in the corroded layer. High-temperature strengths after exposure did not change, because the crack disappeared by melting of the corroded layer.

(3) A model was proposed for the relation between defect formation and strength after exposure in corrosive environments at high temperature. The model was consistent with fracture behavior of ceramics in this study.

2.9.5 Corrosion Test of Si_3N_4, SiC in High-Temperature, High-Speed Combustion Gas Flow

43070054AAA Tokyo FINE CERAMICS in English Mar 93 p 857

[English abstract of article by S. Umebayashi, K. Kishi, K. Miyazaki, and H. Yoshida, Government Industrial Research Institute, Kyushu]

[Text] A very small amount of particles feed into combustion gas flow and was considered for corrosion testing of Si_3N_4 and SiC in high-temperature, high-speed combustion gas flow with fine particles. Corrosion tests of two kinds of Si_3N_4 (SN-A and B) and SiC (SC-A and B) materials developed in this project were done.

The testing condition for them are as follows:

Temperature: 1250°C (SN-A), 1400°C (SC-A, SC-B, SN-B)
Atmosphere: Combustion gas of butane and air
Gas velocity: Above 200 m/sec
Sort of particle: Coal ash
Amount and size of particle: 0.05 mg/Nm^3, Less than 10 μm
Exposure time: 200h

The samples after test are required to satisfy the following demands:

1) Surface roughness: Less than 12S
2) Strength: No degradation
3) No pit formation which decrease strength by oxidation
4) No pit formation which decrease strength by attack of coal ash

1) Coal ash was put on a sand bed (about 200 μm ϕ)/a layer of glass beads (2 mm ϕ)/a glass filter in plastic cylinder (40 mm ϕ x 150 mm long). Dry air was introduced into the cylinder from the bottom of it through a glass filter. Sands formed a floating layer by air through the glass filter and a layer of glass beads unraveled coal ash agglomerate to very fine particles and they floated in air and went into combustion gas by the amount of 0.04 mg/Nm^3 continuously.

2) Surface roughness of the samples exposed in combustion gas atmosphere with coal ash increased after test, because the glassy phase on the samples reacted with coal ash to decrease the viscosity of it and moved away with gas flow.

Surface roughness of SN-B, SC-A, and SC-B are less than 12S and SN-A is more than 12S. Fracture surface of SN-B, SC-A, and SC-B showed no pit formation by attack of coal ash and oxidation under high-temperature high-speed gas. On the other hand, the surface of SN-A was eroded by the depth of about 40 μm. Fracture origins of SN-B, SC-A and SC-B after tests were interior defects and surface defects in SN-A caused by erosion of oxidation layer. Strength of SN-B, SC-A, and SC-B after test was approximately the same as before the test and strength of SN-A after test decreased to 90% of original strength.

2.9.6 Thermal Fatigue Behavior

43070054BBB Tokyo FINE CERAMICS in English Mar 93 p 868

[English abstract of article by Nobuo Ayuzawa and Masamichi Takai, New Materials Research Center, Shinagawa Refractories Co., Ltd.]

[Text] The objective of this study is to investigate the thermal fatigue behavior of the developed materials of silicon nitride and silicon carbide in relation to some properties after thermal cycling and heat treatments in some gaseous environments. JIS standardized and hollow cylinder shaped specimens were examined under thermal cyclic and heat treatments in gaseous environments such as H_2, CO, CO_2, N_2, and air.

The results obtained are summarized as follows:

1. Developed material of silicon nitride has good thermal fatigue behavior on thermal cycling tests. Fracture strength of this material before and after thermal cycling of 10^3 cycles in air and N_2 at 1250°C are 1,040MPa, 960MPa, and 1,020MPa, respectively. It shows this developed material has good properties and usable material for high-temperature applications.

2. Developed materials of silicon nitride and silicon carbide were heated in gaseous environments such as H_2, CO, CO_2, N_2 and air and these materials are affected on weight, phase components, microstructure, and strength. It was clear that active oxidation occurred during H_2, CO gas exposure, and resulted in weight loss and degradate strength. Nevertheless these results, developed materials have high fracture strength after gas exposure and good corrosion resistance, it is considered these materials have good high-temperature properties.

3. Development of Toughness Reinforced Materials Technology

3.1 Particle Dispersion High-Toughness Materials

3.1.1 Particulate-Reinforced Silicon Nitride Materials

43070054CCC Tokyo FINE CERAMICS in English Mar 93 p 889

[English abstract of article by Akio Yoshida, Kei Isozaki, and Yukihiko Nakajima, Denki Kagaku Kogyo Co., Ltd., Omuta Plant]

[Text] In this research, toughening effects of microstructure of sintered bodies and dispersed particles in silicon nitride materials were investigated in order to achieve the target values of $K_{IC} \geq 12MPam^{1/2}$ and $\sigma_{1350}°C \geq 600MPa$. The obtained results are summarized as follows.

The fracture toughness of the materials was found to be largely influenced by the Si_3N_4 grain size from the result of quantitative analysis of the microstructure of sintered bodies. Although the fracture toughness increased with increases in Si_3N_4 grain size, it did not increase in the range of some large grain size. The controlling method of microstructure giving high fracture toughness was developed by examining the sintering process (gas pressure/HIP).

The maximum value of $11MPam^{1/2}$ was obtained at a small amount of TiN addition as a result of the examination of some kinds of dispersed particle (TiN, SiC, Cr_3C_2) using the gas pressure/HIP sintering method. The Si_3N_4 grain size decreased with increasing amount of dispersed particles. Therefore, the balance of the toughening effects of the Si_3N_4 grain and dispersed particles is very important to develop highly toughened particulate-reinforced silicon nitride materials.

3.1.2 Research on Particle Dispersed Silicon Nitride of High Fracture Toughness

43070054DDD Tokyo FINE CERAMICS in English Mar 93 p 912

[English abstract of article by Takashi Matsuura, Jinjoo Matsui, Hisao Takeuchi, and Akira Yamakawa, Itami Research Laboratories, Inorganic Materials R&D Department, Sumitomo Electric Industries, Ltd.]

[Text] The fabrication process and microstructure of Si_3N_4-based nanocomposites were investigated for the improvement in fracture toughness. the fine silicon nitride powder containing metal nitride particles such as VN, NbN, TaN, and TiN were synthesized by heating the mixtures of Si_3N_4 and corresponding metal oxide powders in a N_2 atmosphere. the obtained VN/Si_3N_4, and TiN/Si_3N_4 powders were confirmed to be very fine (20 to 30 nm in diameter). These composite powders were sintered with sintering aids. no improvement in fracture toughness for the VN/Si_3N_4 composites. For the TiN/Si_3N_4 composites, nano-sized TiN grains were partially dispersed within the Si_3N_4 matrix grains. The fracture toughness was increased in the region where some of the TiN dispersants were incorporated in the Si_3N_4 grains. In order to fabricate uniform TiN/Si_3N_4 nanocomposites structure. Ti containing Si_3N_4 polysilazane was also investigated.

3.1.3 Silicon Carbide Matrix

43070054EEE Tokyo FINE CERAMICS in English Mar 93 p 928

[English abstract of article by Hiroshi Hashegawa and Kagetaka Ichikawa, Showa Denko K.K.]

[Text] The mixed powders of commercially available SiC and TiC powders (mixed powders) with a range of TiC from 0 to 40%vol. were hot-pressed with the addition of B-C and Al-C aids, respectively. Only the body produced by the addition of Al-C aids (Al-C body) was densified within TiC 10%vol. content. The mechanical properties (fracture toughness (: K_{IC}), flexural strength at room temperature ($\sigma_{R.T.}$) and at 1400°C (σ_{1400})) for the bodies produced by the addition of B-C and Al-C aids, respectively, were measured. As a result, it was found that the Al-C body had a higher K_{IC} and $\sigma_{R.T.}$ and lower σ_{1400} than the B-C body, and the K_{IC} of the B-C body increased with the TiC content and the σ_{1400} of the B-C body increased with the TiC content and the σ_{1400} of the B-C body maintained a level similar to the $\sigma_{R.T.}$ within a TiC 30%vol. content. Considering both K_{IC} and σ_{1400}, it seemed that the B-C body with TiC 30%vol. was the best material. As a result of investigation of fracture surfaces, it was found that the toughness was caused by intergranular-fracture.

The reason for the high toughness of the bodies produced by SiC-TiC composite powders was studied. The structures of both bodies produced by the composite powders and the mixed powders of commercially available SiC and TiC powders were investigated. The fracture toughness increased with the growth of matrix (SiC) grains in both bodies. It was considered that the superior toughness of the bodies produced by the composite powders was due to the dispersion of carbon grains or the existence of a grain boundary phase.

3.1.4 Toughening Behavior of Dispersion-Reinforced Silicon Carbide

43070054FFF Tokyo FINE CERAMICS in English Mar 93 p 938

[English abstract of article by Tesuro Nose, Jiro Kondo, Shigeharu Matsubayashi, and Hiroshi Kubo, Advanced Materials and Technology Research Laboratories, Nippon Steep Corp.]

[Text] Particle dispersed ceramics are well known to exhibit relatively high fracture resistance. Many investigations have been conducted to examine the toughening behavior in such ceramics. However, the toughening mechanisms have not yet been clear. The purpose of this report is to obtain an analytical expression describing the relationship between the improvement in fracture toughness and the physical properties of both particle and matrix in the system of particulate-reinforced ceramic-matrix composites.

Investigations are based on the analysis of the effect of residual stress on fracture toughness. Residual stress, which may relax the internal stress in the region of the crack tip, occurs due to a mismatch of the thermal expansion coefficients between the matrix and the reinforcement particles. The theoretical analysis indicates that the improvement in the critical stress intensity factor is proportional to the residual stress and the square root of the average particle size. To confirm the analytical results, experimental studies are carried out in fully dense $SiC-Al_2O_3$ and Al_2O_3-SiC composites in various compositions and particle sizes. It exhibits that the theoretical analysis can give enough of a prediction to the experimental results.

Based on the analysis, $SiC-TiB_2-HfC$ ceramics are proposed as a high fracture toughness and high strength SiC-matrix composite. Fracture toughness of $7.2MPam^{1/2}$ at R.T. and tensile strength of 430MPa at 1,673 K are recorded successfully in the hot-pressed $SiC-TiB_2-HfC$ composite.

3.1.5 Effect of Metallic Boride Addition on Fracture Toughness of SiC-B-C Ceramics

43070054GGG Tokyo FINE CERAMICS in English Mar 93 p 958

[English abstract of article by Hiroshi Kubota and Shumei Hosokawa, Krosaki Corp.]

[Text] Improvement of fracture toughness for silicon carbide composites containing 15vol% dispersed transition metal boride particles was investigated. The fracture toughness for SiC and MoB_2 composites incorporating Al and CrB_2 was $4.7MPam^{1-2}$, an increase of a factor of two over monolithic SiC-B-C. Increased fracture toughness in these SiC-MoB_2 composites depended on acceleration of intergranular fracture which was caused by control of interfacial properties.

The SiC-SiC interfacial structure was modified by Al addition which had the effect of altering the fracture mechanism from an intragranular to an intergranular mode in the SiC matrix. Formation of an MoB_2-CrB_2 solid solution from MoB_2 and CrB_2, introduced residual higher thermal stresses at the SiC, MoB_2-CrB_2 interfaces in SiC-MoB_2-CrB_2 composites than at the SiC, MoB_2 interfaces in SiC-MoB_2 composites. Increasing residual thermal stress caused reduction in the bonding strength at the SiC and MoB_2-CrB_2 interface and had the effect of accelerating the debonding of the SiC, McB_2-CrB_2 interfaces.

3.2 Fiber-Reinforced High-Toughness Materials

3.2.1 Development of SiC Whisker Reinforced Si_3N_4 Matrix Composites

43070054HHH Tokyo FINE CERAMICS in English Mar 93 p 981

[English abstract of article by Takayuki Fukasawa, Yasuhiro Goto, Masahiro Kato, Toshiaki Mizutani, Shunichiro Tanaka, and Akihiko Tsuge, Toshiba Corp., R&D Center]

[Text] SiC whisker reinforced Si_3N_4 has been investigated to improve fracture toughness and high-temperature mechanical properties. It is important to analyze basic fracture behavior in developing the high-toughness material. The load-displacement curve was measured precisely for CN (Chevron Notch) specimen to evaluate effective fracture energy, γ_{eff}. It was noted that γ_{eff} was affected by sintering temperature, and that composites had a higher γ_{eff} than monolithic Si_3N_4, sintered particularly at high temperatures.

R-curve behavior was measured by the indentation strength in bending (ISB) method. Increases in the initial fracture resistance with the sintering temperature and remarkable rising in the R-curve for whisker composites were detected.

The contributions of grain growth in Si_3N_4 matrix and those of SiC whisker to fracture behavior were clarified. The effects of whisker on the fracture strength at high temperature were also reviewed. It was found that the whisker in gas-pressure sintering process acted as an inhibitor of Si_3N_4 grain growth and minimized the degradation of strength. Furthermore, SiC platelet was effective on improving the fracture resistance even if it decreases the strength. Based on these results, SiC whisker and platelet reinforçed Si_3N_4 was developed using the gas-pressure sintering process, which had 10.3 ±1.4MPam$^{1/2}$ in K_{IC} and 476 ±34MPa in fracture strength at 1250°C.

The whisker coating technologies were developed, such as the sputter, plasma CVD and sol-gel methods, in order to control the whisker/matrix interfaces.

The result of the push-out test suggested that a hard interfacial bonding such as Ti coating could improve the fracture behavior. It was also recognized that Ti coating the whisker enhanced fracture toughness. But it is not enough to analyze the interfacial affairs, which will be important in further research.

The technique of evaluating residual strength was also developed and it can be available to be clear a toughened mechanism.

3.2.2 Development of SiC Whisker-Reinforced SiC Ceramics

43070054III Tokyo FINE CERAMICS in English Mar 93 p 1013

[English abstract of article by Kaoru Miyahara, Takashi Sugita, Katsumi Takahashi, Shin Koga, and Tadashi Sasa, Research Institute, Ishikawajima-Harima Heavy Industries Co., Ltd.]

[Text] The mechanical properties of SiC whisker-reinforced SiC ceramics developed in this project were evaluated in respect to structural characteristics and process parameters. The following results were obtained:

• Fracture toughness of the composites increased with the thickness of carbon layer, which was introduced by CVD coating process, between the whisker and the matrix. The optimum amount of the coating was studied, and lower CVD temperature tended to give higher toughness.

• Bending strength and Young's modulus were found to decrease with thickness of the carbon layer probably due to the reduced load transfer through the weak carbon interfaces.

• The effect of whisker diameter on the toughness was also investigated. The highest toughness was obtained at diameter of about 2.5 micrometer.

• As a result of the toughness measurements of the composites densified at different temperatures, higher densification temperature was confirmed to reduce the toughness. This implies whisker degradation at high temperature, and lowered sintering temperature is necessary to obtain desired high toughness.

Fracture toughness and R-curve behavior was measured for the composites fabricated by the optimized conditions. composites with unidirectional orientation of whiskers achieved by extrusion showed toughness of $7.5 MPa \cdot m^{1/2}$ and fracture resistance of $8.5 MPa \cdot m^{1/2}$. Microstructural observation revealed such toughness increase corresponded to the density of whisker bridging on the fracture surfaces.

3.3 Estimation of Mechanical Properties

3.3.1 Fracture Behavior Under Tensile and Combined Stresses

43070054JJJ Tokyo FINE CERAMICS in English Mar 93 p 1024

[English abstract of article by Y. Nakasuji, T. Makino, H. Iwasaki, S. Shimada, N. Yamada, H. Sakai, M. Masuda, and M. Matsui, NGK Insulators, Ltd.]

[Text] In order to clarify the influence of mechanical and environmental factors on the strength properties of toughened material and surface-reinforced material developed in this project, different types of fracture tests were carried out.

Strength of toughened materials and surface-reinforced materials were evaluated in air and inert atmosphere at room and elevated temperatures. A tensile strength test using a button-head type small size specimen was developed in order to evaluate the tensile strength of toughened materials. Silicon nitride matrix materials showed strength degradation at an elevated temperature, but silicon carbide matrix materials did not show that characterization. The tensile strength in inert atmosphere was similar to the strength in air. The influence of oxidation on tensile strength is small. Crack growth behavior of toughened materials was evaluated by the dynamic fatigue test. Toughened materials showed larger strength degradation than monolithic materials with a decreasing stress rate. Oxidation has great influence on the slow crack growth behavior. It is effective to suppress the oxidation by coating technique. The fracture toughness of toughened materials was improved in comparison with monolithic ceramics. A fracture test under contact stress of toughened materials and surface-reinforced materials were evaluated by the pin-on-disk test. Fracture resistance for contact stress was improved in comparison to that of the monolithic material. This is because the toughened materials have a larger resistance to crack growth and surface-reinforced materials have a larger relaxation of contact stress at the coating layer.

3.3.2 Impact Fracture

43070054KKK Tokyo FINE CERAMICS in English Mar 93 p 1061

[English abstract of article by Tatsuya Yamada, Japan Fine Ceramics Center]

[Text] In this period, a measuring method was established for the dynamic fracture toughness value of fast propagating crack, K_{ID} using pulsed holographic microscopy. Using a drop-weight type impact testing apparatus, the dynamic fracture toughness value of K_{ID} of monolithic ceramics (silicon nitride, alumina) and ceramic composites (CFRSN: unidirectional carbon-fiber reinforced silicon nitride) were measured at room temperature.

In the case of monolithic ceramics, it was found that the value of K_{Id} depended on the increase rate of $K_{ID}(dK_{Id}/dt)$.

On the other hand, we also found it is not suitable for measuring the strength and K_I-value of CFRSN.

We have applied the pulsed holographic microscopy technique to measure the COD (crack opening displacement) of a fast propagating crack in ceramics for estimating the value of K_{ID}. Using this technique, a microphotogram of the propagating crack was taken, and the K_{ID} values of silicon nitride were estimated.

3.3.3 Erosion Properties of Composite Ceramics

43070054LLL Tokyo FINE CERAMICS in English Mar 93 p 1082

[English abstract of article by Mikio Iwasa and Makoto Kinoshita, Government Industrial Research Institute, Osaka]

[Text] Particle and whisker dispersion was investigated to improve the fracture toughness and other properties of monolithic ceramics. Four kinds of composite materials developed through this project were subjected to the erosion test: particle dispersed silicon nitride (SN/P), whisker reinforced silicon nitride (SN/W), particle dispersed silicon carbide (SC/P), and whisker reinforced silicon carbide (SC/W). The erosion tests were conducted under the same procedure shown in Section 2.9.3.

The erosion volume calculated from wear scar was fairly proportional to the weight loss, which means that we can precisely estimate the erosion wear of composite materials either from erosion volume or from erosion weight.

The erosion wear of composite materials and their dispersion were considerably greater than those of monolithic ceramics. SN/W showed twice and SN/P several times greater erosion than that of monolithic silicon nitride. SC/P showed ten times and SC/W more than twenty times greater erosion. Some improvements must be made for erosion-resistant applications of composite materials.

4. Design Guide for Ceramic Components

43070054MMM Tokyo FINE CERAMICS in English Mar 93 p 1084

[English abstract of article by Akihiko Suzuki, Research Institute, Ishikawajima-Harima Heavy Industries Co., Ltd.]

[Text] During the first to third stages of this project, efforts were made to develop a design guide for ceramic components. There were no design guides or codes like the one developed here in the world, which has a well-regulated theoretical foundation and wide applicability. But there are still several points to be further examined. One of those points is the verification of the design guide. Therefore, in the generalized evaluating stage of the project, some experimental and theoretical verifications of the design guide were conducted, including the generalized evaluation test of model specimens of ceramic turbine components at 1400°C of TIT. Through these verifications and necessary improvements of the text of the design guide, such as including the idea of the inherent strength of the material, improvement in estimating the fatigue life at high temperature and the adoption of an elaborate estimation method of the strength in the multiaxial stress state, the design guide is finally settled during the generalized evaluating stage of the project and a document is issued including the text of the design guide and its explanations. The proposed design guide can be applied to ceramic components preventing fast fracture as well as time-dependent fracture. It can also be applied to design ceramic components which are to be subjected to proof testing.

Chapter III. Basic Research

1. Manufacturing Process Technology

1.1 Evaluation of Process Technology

1.1.1 Microstructure and Fracture Toughness of Silicon Nitride Ceramics

43070054NNN Tokyo FINE CERAMICS in English Mar 93 p 1113

[English abstract of article by Takaaki Nagaoka, Koji Watari, and Shuzo Kanzaki, Government Industrial Research Institute, Nagoya]

[Text] Silicon nitride ceramics with different grain morphology and fracture toughness were prepared by sintering at 1900°C for 2 to 24h in an N_2 atmosphere of 0.9MPa. Two- and three-dimensional (2-D and 3-D) distributions of grain size and aspect ratio were analyzed to clarify the relationship between microstructure and fracture toughness. The 2-D and 3-D grain size distributions were in good agreement. However, the 3-D aspect ratio distribution curve shifted toward the higher value with a broader distribution as compared with that of 2-D.

The improvement in fracture toughness was attributable to the increase in the volume and number fractions of grains in a particular elongated grain group (grain size: 1 to 1.5 μm, aspect ratio: 4 to 8) in the 3-D distribution. The increase in fracture toughness was also explained by the increase in the area and number fractions of grains in a particular grain group modified in the 2-D distribution.

1.1.2 Sintering Behavior of α' - β' Sialon Ceramics and Evaluation of Its Grain Boundary Phase

43070054000 Tokyo FINE CERAMICS in English Mar 93 p 1123

[English abstract of article by Koji Watari, Takaaki Nagaoka, and Shuzo Kanzaki, Government Industrial Research Institute, Nagoya]

[Text] The sintering behavior of α'-β' sialon ceramics with AlN and oxides (Y_2O_3, Er_2O_3, and Yb_2O_3) was investigated by high-temperature dilatometry and microstructural observation. The densification of α'-β' sialon ceramics progressed by particle rearrangement and solution-reprecipitation processes with a transient liquid phase. The shrinkage started around 1200°C, and the shrinking rate was increased by increasing the sintering temperature, but was reduced due to the formation of α'-sialon. Thereafter, the densification proceeded through the dissolution of α'-sialon and remaining α-Si_3N_4 into the liquid phase and reprecipitation of β' grains. At the final stage of sintering, the shrinkage rate decreased due to the growth and interlocking of a large amount of β' grains with prismatic shape. The type of oxides influenced strongly the sintering behavior and phase composition, and the densification and reactions from α-Si_3N_4 to α', and from a' and α to β' accelerated in order of $Y_2O_3 > Er_2O_3 > Yb_2O_3$ addition. The liquid temperature and viscosity of liquid phase formed decreased in order of $Y_2O_3 < Er_2O_3 < Yb_2O_3$ addition. The result of low temperature specific heat measurement suggested the existence of a small amount of grain boundary glassy phase in the α'-β' sialon ceramics. Also the behavior of internal friction for α'-β' sialon was similar to that of one for silicon nitride without additive.

1.2 Machining Technology for Ceramics (High-Quality Grinding of Ceramics With Very-Fine-Grained Wheel)

43070054PPP Tokyo FINE CERAMICS in English Mar 93 p 1138

[English abstract of article by Keisaku Okano and Chisato Tsutsumi, Mechanical Engineering Laboratory]

[Text] High-quality machining technology is very important especially for ceramics, since the strength of ceramic materials is profoundly affected by microcracks and roughness formed on the surface due to the machining process. Machining performance in grinding of ceramics to obtain high-quality ground components has been investigated experimentally.

The newly developed electrochemical in-process dressing method was applied to finer grain-size wheels for a finishing mirror-like surface in the contour grinding of a blade-shaped silicon nitride with a machining center. The in-process dressing enabled a fine grain-size wheel to keep almost constant normal force during grinding.

The relationship between the grain size and the surface roughness of the ground ceramics was determined. A high-quality surface (Ra-0.005 μm) could be accomplished with silicon nitride by using a 10,000-mesh metal-bonded diamond wheel. The X-ray diffraction measurement showed that the surface compressive residual stress increased with increasing feed rate or decreasing wheel speed. It is concluded that the residual stresses decrease with decreasing chip cross-sectional area.

1.3 Shock Consolidation and Shock-Activated Sintering

43070054QQQ Tokyo FINE CERAMICS in English Mar 93 p 1152

[English abstract of article by Kunio Kamiya, Fumikazu Ikazaki, Kunio Uchida, Mitsutaka Kawamura, Katsumi Tanaka, Katsutoshi Aoki, and Shuzo Fujiwara, National Institute of Materials and Chemical Research (formerly the National Chemical Laboratory for Industry)]

[Text] Direct shock consolidation and shock-activated sintering of Si_3N_4 was conducted mainly by the use of one-dimensional explosive shock treatment. Sintering characteristics were examined in the following procedure. Shock compacted silicon nitride was first deagglomerated and mixed with sintering aid additives, followed by firing.

The following were the results induced:

(1) Shock-activated silicon nitride was easily decomposed at sintering temperature because of activated surface. Sintering under high pressure of nitrogen gas prevented the shock-activated silicon nitride from being decomposed.

(2) Effect of shock treatment on the sinterability of Si_3N_4 with 5 wt% Al_2O_3 and 2 wt% Y_2O_3 (5Y2A) depended on the properties of Si_3N_4; shock-treated silicon nitride manufactured by nitridation of silica (sample A) had better sinterability than intact powder but the shock-treatment degraded sinterability in the case of silicon nitride manufactured by direct nitridation of metal silicon (sample D). In the former case, the relative density of the sintered body was as high as 95% at 1550°C by hot press. The reason why shock-treated sample A had better sinterability was considered to be a higher green density before firing probably due to destruction of strong agglomerates by the shock compaction. Sintering characteristics of shock-activated silicon nitride matrix and silicon carbide whisker was also investigated using 5Y2A as sintering aid additives. The results were almost the same as those of the shock-activated silicon nitride with 5Y2A above described.

(3) Fracture toughness was not different between intact and shock-activated silicon nitride.

(4) Stepwise shock pressure increased method was developed. The method consisted in putting buffer plates such as copper, PMMA and aluminum between explosives and the sample holder. The method could prepare a shock compact of relative density of ca. 67% without macrocrack, but still some microcrack existed.

(5) Direct compact of model tube was conducted by two-dimensional shock assembly. In the case of using low melting temperature alloy as a mandrel, a pretty good tube was produced.

1.4 Toughness Reinforced Materials Technology

1.4.1 Effect of Dispersed Particle Size on Mechanical Properties

43070054RRR Tokyo FINE CERAMICS in English Mar 93 p 1171

[English abstract of article by Masaki Yasuoka, Kiyoshi Hirao, and Shuzo Kanzaki, Government Industrial Research Institute, Nagoya]

[Text] Alumina or mullite ceramics with 10 vol% nonoxide particulates were hot pressed at 1500°C for 2 hours in N_2 under a pressure of 40MPa, and the effect of dispersed particle size on mechanical properties was investigated. Compared to monolithic ceramics, the flexural strength for most of composites increased when the dispersed particle size was small. The fracture toughness of composites was found to be directly related to the difference in thermal expansion coefficients between matrix and dispersed particle. These results are explained as follows. The increase in fracture toughness is caused by microcracking originated by differences in thermal expansion between matrix and dispersed particle. In the case where the difference of thermal expansion and the size of dispersed particle are large, cracks arise spontaneously during cooling releasing thermal stress; hindering, in this way, the operation of the microcracking mechanism to increase fracture toughness of the composites. It is concluded that a suitable size of dispersoids existed in each system. On the other hand, the rise of strength is caused by the increase in fracture toughness and by the decrease in a length of preexisting crack due to a suppression of abnormal grain growth.

1.4.2 Fiber-Reinforced Ceramics

43070054SSS Tokyo FINE CERAMICS in English Mar 93 p 1183

[English abstract of article by Kazuo Ueno and Makoto Kinoshita, Government Industrial Research Institute, Osaka]

[Text] The manufacturing process technology and the basis of toughening mechanism were studied to fabricate silicon carbide whisker/silicon nitride matrix composite with optimum properties. The matrix Si_3N_4 grain structure is affected by the whisker incorporation. It is necessary to select sintering conditions which allow the optimum matrix toughness by elongated beta grains and the increment by the whisker. Concerning the whisker thickness, there is an appropriate range of the size, that is, 1 to several micrometers which is several times greater than that of matrix grain. Coating of polycarbosilane on whisker resulted with remarkable increase in fracture resistance with long-range crack growth. In-situ observation of the crack propagation showed that large size grain cluster bridging took place which might explain a rising R-curve by the crack growth over several millimeters.

1.5 Surface Strengthening Technology--Surface Modification by MeV Ion Implantation

43070054TTT Tokyo FINE CERAMICS in English Mar 93 p 1199

[English abstract of article by Kazuo Saitoh, Masami Ikeyama, Hiroaki Niwa, Yoshiko Miyagawa, and Soji Miyagawa, Government Industrial Research Institute, Nagoya]

[Text] Effects of MeV ion implantation into hot-pressed Si_3N_4 have been investigated by means of microhardness testing, microscopic observations, surface swelling, and electrical conduction measurements. Dependencies of the surface properties on implantation conditions and the annealing behavior are discussed in relation to the specific feature of irradiation damage.

Variation of microhardness with implantation dose was found to be as a competition between hardening induced by radiation damage and softening due to amorphization of the surface layer. The maximum increase in relative hardness was about 10% for Si implantation at room temperature.

Microscopic observations of surfaces Si-implanted more than 10^{17} ions/cm^2 at 100 K have shown that amorphization and softening of surface layer led drastic changes of surface morphology, depending on the implantation energy.

Surface swelling measurements have given a sensitive measure of surface compressive stress and/or damage level at low doses. Main feature of the surface swelling could be described by a simple consideration of defect creation and its recovery.

Electrical conductivity of Si_3N_4 implanted at high temperature could be measured at a wide range of implantation dose, and it was proportional to the dose. It was suggested that the conduction is related to some irradiation damage.

2. Evaluation of Products Characteristics/Sintered Body

2.1 Strength (Fatigue Property)

43070054UUU Tokyo FINE CERAMICS in English Mar 93 p 1215

[English abstract of article by Yukihiko Yamauchi and Tatsuki Ohji, Government Industrial Research Institute, Nagoya]

[Text] Fatigue tests were carried out on several structural ceramics and, firstly measured bending fatigue behaviors were compared with the lifetime predicted from the dynamic fatigue properties. Experimental results indicated that a delayed failure of ceramics under a cyclic loading was caused mainly by extension of a preexisting flaw and the lifetime was substantially predictable from a subcritical crack growth behavior. It was also pointed out that at elevated temperatures the crystallization of glassy phase at grain boundaries extended the lifetime and that a crack growth was accelerated by compressive stress if grain (cluster) bridgings and/or crack interlockings were formed on a crack surface.

Secondly, size effect on the fatigue behavior of sintered silicon nitride was discussed. The difference of the room temperature fatigue behaviors estimated by different testing methods could be explained by effective volume of the specimen surface layer of which depth was 100 μm. At high temperature, the difference could be substantially explained by the effective volume of the whole of specimen, but, in spite of the data correction by effective volume, the tensile fatigue data did not agree with the bending one in low stress region. The difference of the cavitation effects on the crack growth properties under the bending and tensile loading conditions was considered as the possible reason of the disagreement.

2.2 Corrosion Test of Si_3N_4 and SiC in High-Temperature, High-Speed Combustion Gas Flow

43070054VVV Tokyo FINE CERAMICS in English Mar 93 p 1235

[English abstract of article by S. Umebayashi, K. Kishi, K. Miyazaki, and H. Yoshida, Government Industrial Research Institute, Kyushu]

[Text] Si_3N_4 (additives: Y_2O_3, ZrO_2, MgO) coated with chemical vapor deposition (CVD) Si_3N_4 and CVD SiC, SiC (Al_2O_3) fabricated from high purity SiC powder developed in this project and β-sialon with Z=0.5 in Si_6-zAlzOzN_8-z (Z=0-4.2) fabricated from α-Si_3N_4 and $Al(OC_3H_7)_3$ solution were exposed in combustion gas atmosphere at 1200°C and 1300°C with gas velocity of 185 m/sec and 235 m/sec, respectively, in exposure time of up to 200 hours which simulate gas turbine engine operating conditions.

Si_3N_4 (Y_2O_3, ZrO_2, MgO) was so hardly oxidized and attacked by gas flow that the strength of it dropped to 50% of its original strength. By coating CVD Si_3N_4 and SiC film on the Si_3N_4 (Y_2O_3, ZrO_2, MgO), the oxidation resistance of it was so much improved and no degradation in strength of coated samples occurred after the exposure test.

In SiC (Al_2O_3), some bubbling of glassy phase in the oxide layer on SiC (Al_2O_3) from SiC powder commercially available was observed and some degradation of strength after testing occurred. In the oxide layer on SiC (Al_2O_3) from high purity SiC powder, there was no bubbling and very small pores (2~3 μm) by formation of CO gas were found. No decrease in strength occurred after testing.

The oxidation resistance of β-sialon from α-Si_3N_4 and $Al(OC_3H_7)_3$ is much better than β-sialon commercially available and β-sialon from Al_2O_3 powder.

The strength of β-sialon varied from 600MPa to 1300MPa depending on the surface treatment.

They dropped to 430MPa after the 100-hour exposure test. In samples which showed degradation of strength after testing at 1200°C and 1300°C, concave areas of fracture origin were found on the surface exposed to the combustion gas flow. This was considered to be formed by chipping of the area (to which iron oxide from the burner nozzle stuck) on rapid heating and cooling at the start and stop of the testing apparatus.

2.3 Tribological Properties of Ceramics

43070054WWW Tokyo FINE CERAMICS in English Mar 93 p 1249

[English abstract of article by Mikio Iwasa and Makoto Kinoshita, Government Industrial Research Institute, Osaka]

[Text] The friction and wear properties of ceramics will change according to the environment or conditions under which they are used. It is indispensable to measure friction and wear under various conditions as will be expected for applications of engineering ceramics.

First, the effects of liquid environment were investigated by the ball-on-disk testing method. The friction and wear of ceramics were greatly reduced in alcohol compared with those in air. In water, friction was usually reduced, but wear was increased in some cases perhaps by the tribochemical effects.

The hard particles added to liquid environment considerably increased wear of ceramics by abrasion effects, but friction was not changed.

The erosion wear of ceramics was also measured by the silicon carbide-particle impingement method. The erosion rate was greatly reduced with increasing hardness and fracture toughness of ceramics.

The solid lubricants such as MoS_2, BN or SiC were incorporated to alumina ceramics by the hot-pressing process, and the effects on tribological properties were investigated. Though the friction was not changed, the wear was rather increased, if much lubricant was incorporated. The erosion wear was also increased. The densification processes and testing conditions must be reconsidered for the improvement of the tribological properties.

2.4 Toughness

43070054XXX Tokyo FINE CERAMICS in English Mar 93 p 1260

[English abstract of article by Shuji Sakaguchi, Norimitsu Murayama, and Fumihiro Wakai, Government Industrial Research Institute, Nagoya]

[Text] The aim of this research is to clarify the evaluation method of fracture parameters—such as fracture toughness and fracture resistance—on toughened ceramic materials. We researched six subjects to obtain characteristic parameters of fracture mechanics on ceramic materials. 1) We obtained an equation for the calculation of fracture toughness by chevron notched beam, which can be applied to the JIS type bending bar specimen. 2) We performed indentation fracture test up to 1200°C, and we obtained a new empirical equation for fracture toughness. It has no conflict with the conventional equations for this method, which can be applied only at room temperature. 3) The single edge precracked beam technique is applied for the toughened silicon nitride specimen. R-curve behavior appears during the fracture toughness test. 4) The relation between the stable fracture and oxidation of the whisker reinforced silicon nitride was studied. We assumed that, in a certain condition, oxidation can enhance the toughening mechanism, but we could not find the optimum result. 5) The relationship between the fracture toughness and strain rate was studied. Fracture toughness was independent of the strain rate on silicon nitride. On the contrary, tetragonal zirconia shows large increase of fracture toughness while increasing the strain rate. It is caused by the stress induced phase transformation.
6) R-curve behaviors of three kinds of silicon nitride based ceramics were measured by using single edge notched beam specimens, at room and elevated temperatures up to 1200°C. The rising R-curve is related to the grain size of the silicon nitride, but not to the dispersed secondary phase, such as silicon carbide whiskers.

3. Atomic Structure of Crack Tips in Covalent and Ionic Bond Ceramics

43070054YYY Tokyo FINE CERAMICS in English Mar 93 p 1277

[English abstract of article by Hidehiko Tanaka and Yoshio Bando, National Institute for Research in Inorganic Materials]

[Text] The atomic structure of crack tips in several ceramic crystals was studied in order to investigate the basic brittle nature of high-temperature structural ceramics. The crack tips of covalent bond SiC and covalent-metallic bond Si crystals were found atomically sharp, and there was no dislocation generation associated with the crack tip stress field. The ionic bond MgO, however, generated simple dislocation pairs. These dislocation pairs relaxed I, II, and III modes of the crack tip strain field depending on the combination of their burger vectors. In Al_2O_3 crystal a microcrack was formed by the strain accumulation by basal twins.

Section 2. Summarization of Fine Ceramics R&D (1981~1988)

Introduction

94FE0398C Tokyo FINE CERAMICS in Japanese Mar 93 p 1294

[Introduction to the second section of this publication]

[Text] Finally, the "Fine Ceramics R&D Project," the longest running project since the commencement of the next generation's industrial key technology R&D system, became history. Reports concerning individual research topics up to the second phase and from the third phase to completion were published in "Progress of Next-Generation's Research" in 1992, as well as in the first section of this publication, respectively. In the second section of this publication, the contribution of this project, throughout all the phases to the progress of science and technology of structural fine ceramics, will be reviewed with the summarization of interim and final research achievements for each technical field.

Materials studied throughout the project were limited to silicon nitride and silicon carbide-based materials for both monolithic and toughness reinforcing compound materials. The entire life cycle, from raw material powder synthesis to fracture behavior analysis, of each of these materials was studied. Basically, the R&D technology field was roughly divided into two areas: process technology and evaluation/application technology. R&D concerning individual technology in each area was normally carried out in a parallel fashion, except at the end of each project phase attempts were made to integrate or coordinate technologies belonging to the different areas as much as possible. In the area of process technology, the size of the ceramic material being handled was gradually increased and the shape became increasingly complex, while not losing the sight of achieving target performances; i.e., test specimens were used in the first phase, primary models in the second phase, secondary models in the third phase, and the stator and rotor models in the integrated technology R&D phase. At the same time, in the area of evaluation/application technology, the measurement methods were developed for both time-dependent and time-independent mechanical fracture strength under uni- and multi-axial stress at normal and high temperature regions. The database was compiled based on measurements and analyses of the measurement results. Furthermore, added to this database, in order to establish ceramic component design standards, were the evaluation technologies for the materials' basic properties, performances against various environmental conditions, and the techniques for stress distribution and reliability

analyses. Thus, the above-mentioned models were designed and evaluated during each project phase by using these evaluation/application technologies. With all of these activities constituting the pillars of the R&D plan, the individually developed technologies in the two areas were evaluated from two sides: one standpoint of coping with the integration and interfacing with each other to produce and test the models, and another of having high quality as an independent technology.

After the commencement of the next generation's R&D project, ceramics-related technology development also flourished outside the project and there was epoch-making progress, e.g., the liquid phase synthesis of powder raw materials, the zirconia-based high-strength high-toughness materials, and the long fiber-reinforced ceramic composite materials. At the same time, remarkable improvement was also made in the quality of monolithic silicon nitride and silicon carbide, with their strengths more than doubling the expected values prevalent at the time of the project initiation and with their Weibull constants routinely reaching 20 which had once been a dream. However, there are still problems to be overcome if 100-percent reliability of materials is to be guaranteed in use under anticipated high load, particularly, operation performance of the rotating components: i.e., technologies need to be developed for constructing, for each component, an optimal micro-fine structure that can cope with both large, complex-shape molding and sintering processes; technologies need to be integrated for nondestructive inspection of products; and mechanical grinding operation needs to be minimized or eliminated to simplify the process and also to reduce the cost. We feel as if we just finished only one circle of a spiral staircase in the last 10 years, and we need to start the next circle upward based on the sophisticated quality and technology. It appears that the time is also almost ripe for expanding research into the development of multifunctional materials including inorganic fusion materials.

Chapter I. Process Technology

1. Monolithic Materials

1.2 Forming Process of Monolithic Ceramics

43070054ZZZ Tokyo FINE CERAMICS in English Mar 93 p 1326

[English abstract of article by Takashi Kanno, Asahi Glass Co., Ltd.; Kazunori Koga, Kyocera Co.; Toru Shimamori, NGK Spark Plug Co., Ltd.; Katsutoshi Nishida, Toshiba Co.; and Takeshi Kanda, Kobe Steel, Ltd.]

[Text] In the National Project of Fine Ceramics, three kinds of forming processes, cold isostatic pressing [CIP], slip casting, and injection molding, have been adopted to fabricate the model components corresponding to ceramic gas turbine For the purpose of improvement of characteristics and reliability of ceramic components, the fundamental investigations on the forming of ceramics as well as related powder processing have been carried out.

(1) For the CIP process, the dispersion of powders in liquids was studied on the basis of colloid science, together with characterization of the disperse systems by rheological measurements. The characteristics of spray-dried granules were revealed to control the reliability of sintered ceramics from the experiments by static CIP as well as by cyclic CIP.

(2) For the slip casting process, the dispersion and the rheological properties of disperse systems were studied. Microstructures of slip casted compacts were confirmed the same as those of CIP compacts by the measurements of pore size distributions.

(3) For the injection molding process, the compounding of powders with polymer binders and the rheological properties have been studied in detail.

The fundamental investigations have been applied to the development of the model components of gas turbine stators and rotors. From the flexural strength and Weibull modulus for the testpieces cut from the model components the rupture strength of the model components was estimated by the use of effective volume. The estimated values almost coincided with those measured by thermal shock tests or hot-spin tests for actual model components for gas-turbine stators and rotors.

1.3 Sintering Process of Monolithic Ceramics

43070054AAAA Tokyo FINE CERAMICS in English Mar 93 pp 1367-1369

[English abstract of article by Katsutoshi Nishida and Akihiko Tsuge, Toshiba Corporation; Takeshi Kanda, Tsuneo Tatsuno, and Takao Fujikawa, Kobe Steel, Ltd.; Toru Shimamori, NGK Spark Plug Co., Ltd.; Masaaki Honda, Hisao Takeuchi, and Tomoyuki Awatsu, Sumitomo Electric Industries, Ltd.; Takashi Kanno, Asahi Glass Co., Ltd.; and Kazunori Koga, Kyocera Corporation]

[Text] Development of sintering processing for silicon nitride and silicon carbide ceramics is reviewed for its high-temperature mechanical properties, corrosion resistance, and wear resistance.

1. High-temperature mechanical properties development of silicon nitride

Research and development on sintering of high-strength silicon nitride by means of hot isostatic pressing (HIP) was carried out from 1981 to 1992.

As to the HIP process, capsule-free HIP and "seal + HIP" (glass encapsulation HIP) processes were investigated. In the capsule-free HIP process, the atmospheric effect on high-temperature strength was particularly revealed as the effect on grain-boundary and surface structure. Low nitrogen partial pressure in HIP was effective for obtaining as-HIP high-temperature strength. In the "seal + HIP" process, the most difficult to control was the as-HIP'ed surface condition, because there was the possibility of reaction with glass as a sealant and there was also the environmental effect of reaction barrier inside the glass or grain boundary.

High-temperature strength was closely connected to the structure of grain-boundary, namely its degree of crystallization, characteristics of crystal etc. For an example of this work, high-temperature static fracture and creep rupture strength seemed to be affected by the thin amorphous layer in grain-boundary and such layer seemed to be related to halogen impurities in Si_3N_4 powders.

Improvement of high-temperature properties by grain boundary crystallization is another important technology. Since silicon nitride is fabricated using liquid phase sintering, sintering additives usually remain between Si_3N_4 grains as grain boundary phases. The grain boundary phases are softened and reduce the properties at high temperature. This phenomenon occurs more notably when

grain boundary phases contain glassy ones. We investigated the improvement of high-temperature properties by grain boundary crystallization with no glassy phase. Influences of composition and heat treatment were investigated in the rare earth oxide-alumina system. The internal friction measurement was applied to estimation of grain boundary property at high temperature. Internal friction related softening of grain boundary and highly correlated creep properties. Sintering additives with high liquidus temperature and heat treatment realized complete crystallization and greatly improved creep property.

2. Development of high-temperature corrosion-resistant silicon nitride

Corrosion resistance is one of the most important properties of ceramics in high-temperature application. High-purity silicon nitride has potentially high oxidation resistance; however, impurities included in raw powder and sintering additives have detrimental effect on the properties. The new post-reaction sintering method has been developed for the high-oxidation resistant material.

3. Development of the process for high wear-resistant silicon nitride

The manufacturing process of wear-resistant silicon nitride ceramics was investigated. We investigated structures of silicon nitride proposed for superior characteristics to different types of wear. Sintered bodies of high fracture toughness with fine and homogeneously extending grains were superior both in the friction wear and in the abrasion wear resistance.

Fine and extending grains were more important for friction and abrasion wear resistance, respectively. In order to attain these characteristics, some processes, such as powder treatment, pressure controlled sintering, heat treatment, etc., were developed. Powder treatment by the attrition mill method was effective on homogeneous powder mixing which realized sintered bodies with fine grains. Pressure controlled sintering was effective on homogeneous grain growth. Heat treatment after machining for the purpose of blunting and healing a crack front of the surface microcrack improved wear resistance. On the basis of these investigations, the gas bearing model, the friction wear model, and the abrasion model were manufactured using newly-developed silicon nitride powder in this project. These models have been successfully operating.

4. High-temperature mechanical properties development of silicon carbide

The sintering mechanism of alumina added silicon carbide has been discussed in terms of shrinkage behavior, raw powder properties, phase change during sintering, and microstructure development. The sintering process is divided into three sintering stages, where the initial stage is the densification process by particle rearrangement below 1800°C, the intermediate stage is the sintering process around 1900°C accompanying closed pore formation and the final stage is the densification accompanied by the decrease in the content of closed pores and the particle morphological change from equiaxial to platy. Mechanical properties such as strength delayed fracture and toughness are discussed.

5. Development of high-temperature corrosion resistant silicon carbide

The effect of sintering additives on the oxidation resistance of silicon carbide-Y_2O_3-AlN and silicon carbide-Al_2O_3 systems are investigated. Over 6 wt% of additives are required in the Y_2O_3-AlN system to obtain the same level of strength as that of the Al_2O_3 system. Though the Y_2O_3-AlN system shows relatively high toughness, its oxidation resistance at high temperatures is lower. Thus, alumina is recommended as a sintering additive for high-temperature corrosion resistant silicon carbide.

6. Development of the process for high wear-resistant silicon carbide

High strength and wear-resistant silicon carbide material was developed using pure and fine silicon carbide powder developed in the "Fine Ceramics" project. The size and number of voids were decreased by uniform compaction and densification by CIP and HIP methods, respectively. This caused the increase of strength and Weibull modulus and also the increase of the sliding wear resistance.

Sliding wear resistance was evaluated by a pin-on-disk method with no lubrication.

The achieved characteristics are compared with the project targets.

Items	Unit	Target	Developed SiC
Tensile strength	kg/mm^2	50	59.1
Weibull modulus	—	22	19.4
Sp. wear rate	$10^{-8} mm^3/kg \cdot mm$	1.0	0.6
Surface void diameter	μm	2.0	0.51

7. Characteristic sintering processes development for fine ceramics

As the characteristic sintering processes in the project, the general capsule-HIP ("seal + HIP") process and post-sintering process are introduced along with the characteristic material properties obtained through these processes. Capsule-HIP could produce high strength, high corrosion-resistant silicon nitride without additives; however, the fracture toughness was regrettably comparatively low for structural use, due to the equiaxis microstructure.

The post-sintering technique also has high potentiality to get the above-mentioned properties' silicon nitride ceramics with additives.

As to other sintering processes outside the project, the rapid sintering processes—microwave sintering, plasma sintering, and self-combustion sintering—are briefly reviewed.

2. Development of the Toughened Ceramic Materials

2.1 Particulates and Whisker-Reinforced High-Toughness Ceramic Material

43070054BBBB Tokyo FINE CERAMICS in English Mar 93 pp 1496-1500

[Tables and figures of article by Shuzo Kanzaki, Government Industrial Research Institute, Nagoya; Kazuo Ueno, Government Industrial Research Institute, Osaka; Kaoru Miyahara, Ishikawajima-Harima Heavy Industries Co., Ltd.; Shumei Hosokawa and Hiroshi Kubota, Kurosaki Corp.; Hiroshi Hasegawa, Showa Denko K.K.; Tetsuro Nose, Nippon Steel Corp.; Hisao Takeuchi and Jinjoo Matsui, Sumitomo Electric Industries, Ltd., Akio Yoshida, Denki Kagaku Kogyo Co., Ltd., Omuta Plant; and Takayuki Fukasawa and Akihiko Tsuge, Toshiba Corp.]

[Excerpts]

Table 2.1.1 Properties of Engineering Ceramics

Properties	Silicon nitride			Silicon carbide		Zirconia	alumina	
	reaction sintered	pressureless sintered	hot pressed	reaction sintered	pressureless sintered	partial stabilized	alumina	Al_2O_3-ZrO_2
density(g/cm3)	2.1~2.6	2.9~3.5	2.9~3.5	~3.10	3.08~3.20	5.9~6.1	3.98	4.9
thermal conductivity(w/mk)	2.6~20	13~38	29~32	~200	42~126	1.7~3.3	20	9.2
thermal expansion(x10-6/k)	2.3~3.0	3.0~3.5	~3.2	4.3	4.8~48	8.7~11.4	8.6	9.6
Young's modulus(GPa)	100~200	240~330	320	~420	390~480	150~260	370	320
Poisson's ratio −	0.24~0.26	0.24~0.28	~0.26	~0.24	0.13~0.16	~0.3	−	−
flexual strength(MPa)								
R.T.	150~295	400~1000	800~1050	~530	400~870	700~1000	300~450	1100
1000℃	160~300	350~1000	800~1000	−	−	~500(800℃)	~150	−
1200℃	170~307	250~800	250~950	~530	400~900	~250	−	−
1400℃	−	−	−	−	400~900	−	−	−
fracture toughness(MPa · m1/2)	3~4	4~7	~7	~3.5	2.5~5.6	8~15	2~3	13
thermal shock resistance(RT)(℃)	350~600	400~800	800~900	300~450	300~550	300~550	150~460	~200

Table 2.1.2 Properties of Ceramic Engine Parts

	Parts		Requested properties
Piston-cylinder	Cylinder liner		Abrasion resistance μ <0.05, abrasion <100 μm (Contact stress 20~40MPa) Relative distance 5 x 10^{3}km Thermal expansion coefficient <4x10^6/°C Thermal conductivity ≤0.01cal/cm·s·°C
	Piston head		σ ≥250MPa (600°C) Thermal expansion coefficient <4x10^6/°C Thermal conductivity ≤0.01cal/cm·s·°C Abrasion resistance
	Precombustion part		σ ≥450MPa (1000°C) Thermal expansion coefficient <4x10^6/°C Thermal conductivity ≤0.03-0.06cal/cm·s·°C Thermal shock resistance ≥800°C
	Glow plug		σb ≥ 300MPa Electrically insulating Thermal shock resistance
Moving-valve system	Locker arm		Abrasion resistance Abrasion≥20μm (wet, contact stress 0.5~/GPa)
	Valve guide		Abrasion resistance Refractoriness
	Intake-exhaust valve		σb ≥500MPa (900°C) Thermal shock resistance Abrasion resistance Particulate collision resistance
Ex-changer	Turbo ex-chang-er	Wheel	σb ≥500MPa (1000°C) Creep deformation <1% (5,000hx1000°C) Oxidizing conditions <0.1mg/cm^3 (5,000hx1000°C) Thermal shock resistance ≥800°C
		Housing	σb ≥300MPa Oxidizing conditions <0.1mg/cm^3 (5,000hx1000°C) Thermal shock resistance ≥800°C
Exhaust system	Exhaust port liner		σb ≥300MPa Refractories Thermal expansion coefficient ≤4x10^6/°C Thermal conductivity ≤0.01cal/cm·s·°C
	Exhaust manifold		σb ≥500MPa Refractories (≥1000°C) Thermal expansion coefficient ≤4x10^6/°C Thermal conductivity ≤0.01cal/cm·s·°C

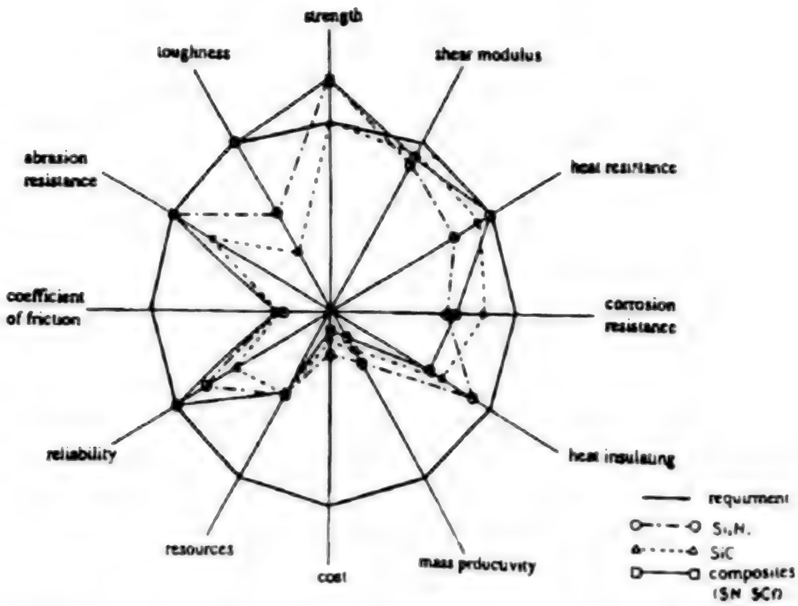

Figure 2.1.1 Application of Ceramics for Engines

Table 2.1.3 Toughening Mechanism

	mechanism	factor
K_{IC}	internal stress 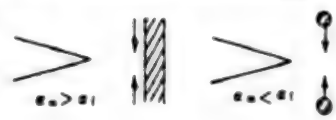	difference in expansion coefficient
	load transfer 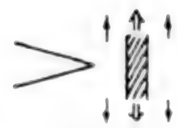	difference in modulus of elasticity
K_R	closure stress 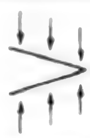	bridging or pullout of fiber and grain
	transformation 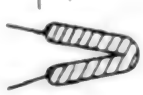	expansion by transfer motion
	microcrack 	micro crack in wake
	mixed mode 	crack deflection

Table 2.1.4 Examples of Composites

Combinations	Examples
Metal/Metal	Metal fiber (or whisker) reinforced metal (FRM), hard metal (W-Ni), bimetal Al wire with steel core
Inorganic/ inorganic	Concrete, mortar, porcelain, pyroceram, glass ceramic, optical fiber, glass (carbon) fiber-reinforced concrete (GF(CF)RC)
Organic/organic	Laminated plastics, wood plastic combination (WPC), organic fiber reinforced plastics, complex fiber, bonded fabric, synthetic leather ABS resin
Metal/inorganic Inorganic/metal	Duralumin, phosphor bronze, sintered aluminum product (SAP) TD-Ni inorganic (or whisker) reinforced metal, cermet
Metal/organic Organic/metal	Vinyl resin coated steel, insulation coated wire, printed wire, LSD, aluminum plastic laminate conductive bond, oilless bearing
Inorganic/organic Organic/inorganic	Safety glass, plastic cement, abrasive, magnetic tape, glass (carbon) fiber reinforced plastic (FRP, FRTP), filler reinforced rubber, formed plastics

Table 2-1-5. Forming Process for Fiber-Reinforced Ceramics

	Forming	[illegible] molding	Fiber
Solid process	Hot pressing (In general) Pressure-less sintering Pressurizing HIP Slip casting-sintering	Mixing Injection molding Slip casting Sol-gel process Slurry	Whisker chopped Whisker chopped short fiber Whisker, preformed Long, short Long
Gas process	CVD, CVI Reaction sintering	Combination of long fiber preformed and Si powder	Preformed Preformed
Others	Melt infiltration (glass etc.) Flame coating		Preformed Preformed

2.2 High-Toughness Ceramics With Controlled Crystalline by Unidirectional Solidification Method

43070054CCCC Tokyo FINE CERAMICS in English Mar 93 p 1578

[English abstract of article by Takashi Kanno, Yutaka Segawa, and Shigemi Katori, Asahi Glass Co., Ltd., Research Center]

[Text]] Development of high-toughness materials was carried out by means of the unidirectional solidification method for eutectic composites such as ZrB_2-B_4C, $ZrO_2(Y_2O_3)$-NiO, $ZrO_2(Y_2O_3)$-CoO and $ZrO_2(Y_2O_3)$-Al_2O_3 systems.

Directional solidification was performed with a floating-zone furnace having halogen lamps in a cavity of dual ellipsoidal reflectors.

Both ZrB_2-B_4C and $ZrO_2(Y_2O_3)$-Al_2O_3 systems yielded aligned structures of ZrB_2 rods in B_4C matrix and $ZrO_2(Y_2O_3)$ rods in Al_2O_3 matrix, respectively, whereas $ZrO_2(Y_2O_3)$-NiO and $ZrO_2(Y_2O_3)$-CoO systems gave lamellar structures of aligned planes. Rod-like structures appeared for the eutectic systems with volume fraction of constituent phase less than 28vol%.

Microstructures were also dependent on the solidification rates. The spacing (λ) of the rods and lamellars decreased with an increasing solidification rate (V), following the relation of $\lambda V^{1/2}$=const.

Fracture toughness (K_{IC}) was measured by the indentation fracture method for longitudinal and transverse sections to the solidification direction.

1) For ZrB_2-B_4C system:
   K_{IC} (transverse) =2.61MPam$^{1/2}$, K_{IC}, (longitudinal)=2.95MPam$^{1/2}$
2) For ZrO_2 (3mol%Y_2O_3)-NiO system anisotropy in K_{IC} was noticeable:
   K_{IC} (transverse) =3.64MPam$^{1/2}$ (parallel to lamella)
   K_{IC} (transverse) =9.49MPam$^{1/2}$ (perpendicular to lamella)
3) For ZrO_2(8mol%Y_2O_3) - CoO system reduction of CoO into Co improved K_{IC}:
   K_{IC} (transverse) =3.75MPam$^{1/2}$ (before reduction)
   K_{IC} (transverse) =4.52MPam$^{1/2}$ (after reduction)
4) For ZrO_2 (Y_2O_3)-Al_2O_3 system crack propagated only along with lamella:
   K_{IC} (transverse) =5.02MPam$^{1/2}$ (parallel to lamella)

Fracture toughness of unidirectionally solidified eutectics was improved as much as 2-9 times compared with those of constituent single crystals.

4. Joining of Ceramics

43070054DDDD Tokyo FINE CERAMICS in English Mar 93 pp 1647-1648

[English abstract of article by H. Takeuchi, Itami Research Laboratory, Sumitomo Electric Industries, Ltd.; and K. Koga, Central Research Laboratory, Kyocera Corporation]

[Text] Joining of both silicon nitride and silicon carbide to each other and to metal was investigated.

A joining method of ceramics to ceramics was developed for the target retaining high temperature flexural strength more than 80% of that of base materials.

As for the silicon nitride materials, the system of silicon nitride-yttrium oxide-alumina was selected for the base material. The sintered silicon nitride material was joined by using the powder mixture of the grain boundary phase composition. The paste of the powder mixture of the grain boundary phase was screen painted on the joining surfaces of the silicon nitride materials. The joining was carried out by firing them in the nitrogen atmosphere and hot isostatic pressing (HIP). Optimizing the conditions, the strength of joined specimen resulted in 800MPa and 640MPa at room temperature and 1250°C, respectively.

Silicon carbide sintered with the addition of both boron carbide and carbon was solid-state-diffusion joined by glass encapsulated HIP. A strength of 450MPa was obtained both at room temperature and 1400°C.

The joining method for the green body developed in the project was adopted to prepare the silicon carbide nozzle ring models for gas turbine bench test. The model was successfully operated at 1400°C.

The ceramics-metal joining method was investigated for the application at high temperature. Chromium-molybdenum steel was selected as the joining metal. The target was 200MPa of joining strength at prescribed high temperatures and 80% of residual strength after 1000 times heat-cycle test. We investigated two factors of ceramics-metal joining: joining interface formation with high strength and thermal stress reduction, especially for improving heat-cycle resistivity.

The joining interface was formed, as for silicon nitride, by multilayer metallizing containing a first layer of titanium using the ion-plating method followed by brazing. As for silicon carbide, an active brazing alloy containing titanium was used. Oxidation resistance was considered in both materials.

As for the stress reduction layer, two types of functions were applied: thermal expansion coefficient (TEC) gradation and plastic deformation. As for silicon nitride, an interlayer combination containing WC-alloy and nickel, applying both functions, was selected. As for silicon carbide, TEC gradation type interlayers which were made of precisely TEC controlled $SiC-TiB_2$ composites developed in this project, were selected.

By these investigations, superior high-temperature characteristics, in both strength and heat-cycle resistance, was obtained. The results were applied to the joining of the silicon nitride bladed disk model and metal shaft for the gas turbine bench test. The model was successfully operated.

5. Surface Strengthening Technology

43070054EEEE Tokyo FINE CERAMICS in English Mar 93 p 1694

[English abstract of article by Kazuo Saitoh, Soji Miyagawa, Yoshiko Miyagawa, Hiroaki Niwa, and Masami Ikeyama, Government Industrial Research Institute, Nagoya; Akihiko Tsuge, Toshiba Co.; and Osamu Sakai, Tomonori Takahashi, Hiroaki Sakai, Takao Soma, and Minoru Matsui, NGK Insulators, Ltd]

[Text] The surface modification by ion implantation and surface coating by chemical vapor deposition (CVD) has been studied in the third and fourth phases of the fine ceramics project as the surface strengthening technology for ceramics. KeV and MeV ion implantation were studied to clarify the effect of the ion implantation to the surface morphology and to the wear resistance of ceramics. The wear resistance of the Si_3N_4 sintered body was improved by ion implantation. CVD surface coating was studied to improve the oxidation resistance and to relax the contact stress of ceramics. Oxidation resistance of the Si_3N_4 sintered body was improved by CVD-Si_3N_4 and CVD-SiC coating.

Chapter II. Evaluation and Application Technology

1. Strength of Structural Ceramics

1.1 Fast Fracture Strength of Structural Ceramics

43070054FFFF Tokyo FINE CERAMICS in English Mar 93 p 1723

[English abstract of article by Y. Nakasuji, N. Yamada, Y. Iwasaki, T. Makino, M. Masuda, H. Sakai, and M. Matsui, NGK Insulators, Ltd.; and S. Hayashi, T. Inamura, H. Baba, and A. Suzuki, Ishikawajima-Harima Heavy Industries Co., Ltd]

[Text] The fast fracture properties of structural ceramics, such as Si_3N_4 or SiC, have been evaluated by various types of testing using simple shape specimens and component modeled specimens, and the theories of the reliability evaluation have been improved. The fast fracture strength of ceramics was evaluated by testing under uniform, nonuniform, and multiaxial stresses at room temperature and high temperature. It was found that the variability of strength was described using the two-parameter Weibull distribution method. The strength of ceramic parts with different size and stress was predicted using the size effect on strength based on Weibull and multiaxial statistical theories. The evaluation method by nonlinear fracture mechanics has been used to describe nonlinearity between strength and crack size, R-curve behavior, and toughening mechanisms.

In order to establish evaluation test methods and design criteria of ceramics for gas turbine applications, fast fracture tests of ceramic model parts were carried out. The tests are the spin test of disks, the tensile test of root parts of axial turbine blade dovetail, the rotary bending test of shoulder rods, the ball on ring test of disks with shoulder fillet, and the combined stress test of blade model specimens. The results of these tests indicated the applicability of the two-parameter Weibull distribution and size effect on strength to the prediction of strength.

1.2 Fatigue Strength of Structural Ceramics

43070054GGGG Tokyo FINE CERAMICS in English Mar 93 p 1761

[English abstract of article by Y. Nakasuji, Y. Iwasaki, T. Makino, M. Masuda, H. Sakai, and M. Matsui, NGK Insulators, Ltd.; and S. Hayashi, T. Inamura, H. Baba, and A. Suzuki, Ishikawajima-Harima Heavy Industries Co., Ltd.]

[Text] Aggressive research and development has raised structural ceramics to a level where they are now of practical use as an alternative to metal. To put structural ceramics to good use for mechanical parts, the parts should have good endurance through practical use. Therefore, various fatigue tests using structural ceramics have been carried out, and fatigue strength on ceramics are gradually cleared

Silicon nitride (Si_3N_4) and silicon carbide (SiC) have the strongest possibility that they will be applied for gas turbine components in structural ceramics. In this paper, fatigue strength on Si_3N_4 and SiC are outlined as follows

(1) Fatigue strength degradation in Si_3N_4 is classified into three mechanisms slow crack growth, creep deformation and cyclic fatigue. For slow crack growth, fatigue strength is predicted by power law for crack growth formula $V=AK_I^n$. For creep deformation, the Larson-Miller parameter is applicable to lifetime prediction. For cyclic fatigue, the failure diagram is proposed for the metal fatigue to show the effects of mean stress and stress amplitude on fatigue strength. This diagram is applicable to decide the safety stress conditions on the parts design using Si_3N_4

(2) Cyclic fatigue failure in SiC is observed at elevated temperature, but not at room temperature Fatigue strength degradation in SiC is due to slow crack growth, so fatigue strength is predicted by power law for crack growth formula $V=AK_I^n$

(3) The unified strength evaluation method is confirmed to be applicable to predict fatigue strength in Si_3N_4 at a certain high temperature

(4) To evaluate fatigue strength concerning ceramic model parts, fatigue tests were performed under multiaxial stresses and concentrated stresses.

1.3 Impact Strength of Ceramic Material

43070054HHHH Tokyo FINE CERAMICS in English Mar 93 p 1801

[English abstract of article by Tatsuya Yamada, Japan Fine Ceramics Center]

[Text] Ceramics have good thermal and mechanical properties for applications of high temperature components, but they show low fracture toughness. So, it is very important to recognize the impact property of ceramics.

In this project, the Japan Fine Ceramics Center has developed two measuring methods for the impact strength, two dynamic fracture toughness K_{Id} and K_{ID}. In this work, two type test systems, a drop-weight type impact testing apparatus and a pulsed holographic microscopy system, were built up to measure these impact properties.

Using the drop-weight type impact testing apparatus, impact strength and K_{Id} of ceramics were measured from room temperature to 1500°C. The strength of ceramics depended on the loading rate, but the K_{Id} did not depend on the loading rate. K_{Id} showed the tendency that is approximately proportional to dynamic stress intensity factor rate $dK_I(t)/dt$.

We have also applied the pulsed holographic microscopy technique to measure the crack opening displacement (COD) of a fast propagating crack in a ceramic specimen to estimate K_{ID}. Using this technique, a microphotograph of propagating crack in gas-pressure sintered silicon nitride specimens were taken and some K_{ID} values of silicon nitride were estimated.

1.4 Fracture Process Analysis of Ceramic Materials by In-Situ SEM Observation and Moire Interferometry

43070054IIII Tokyo FINE CERAMICS in English Mar 93 p 1823

[English abstract of article by Seijiro Hayashi and Isamu Nonaka, Ishikawajima-Harima Heavy Industries Co., Ltd.]

[Text] A scanning electron microscope by which a specimen can be loaded at a high temperature, as high as 1200°C during observation, was developed. To observe crack propagation behavior, a special heating device was attached. Cyclic crack propagation in Si_3N_4 was found to be accompanied by certain types of deformation near the crack tip. All cases of crack propagation under cyclic tension and cyclic tension-compression load were similar in appearance. The enhancing effect of moisture on crack propagation under static load was confirmed by in-situ observation. These results were used to verify the models employed in the design guide and the proof-test guide.

The fracture process zone in Si_3N_4/SiCw ceramic composite was analyzed by a hybrid experimental-numerical procedure employing moire interferometry. The relationship of crack closure stress versus crack opening displacement in the fracture process zone was obtained. It was found that the fracture probability of a component was joint fracture probability of the fracture process zone and the rest of the component outside the fracture process zone. Further studies of the relationship between the R-curve behavior and the Weibull modulus is required for improving the design guide.

3. Evaluation of Ceramic Components

3.1 Nondestructive Inspection Technique

43070054JJJJ Tokyo FINE CERAMICS in English Mar 93 p 1948

[English abstract of article by Yoshinori Tanimoto and Masami Tomizawa, Toshiba Corporation, Fuchu Works; Katsutoshi Nishida and Yutaka Abe, Toshiba Corporation, Keihin Product Operations; and Izumi Tomeno and Hideyuki Oozu, Toshiba Corporation Research and Development Center]

[Text] In comparing the detection of defects for metal at 1 to several millimeters, that for fine ceramics is several tens of microns because of the low toughness of the materials. The requirements of nondestructive testing to detect very small defects in fine ceramics, various kinds of nondestructive testing techniques have been studied but because of the difficulty in doing so, at present such a technology has not yet been established.

In this project, two types of nondestructive testing equipment, the photo-acoustic spectroscope (PAS) and the high-resolution micro focus X-ray CT scanner, were developed for trial use. As a result of their evaluating ability of detecting defects in fine ceramics, first, by PAS, using the test plate with the artificial defects, the defects of which size are approximately 50 μm level were detected. Second, by high-resolution micro focus X- ray CT scanner, the artificial defect (38 μm diameter pinhole) in the 10mm diameter silicon carbide (SiC) test plate could be detected.

Based on the result of the study in this project and literature in Japan and other countries, the study regarding types and features for various kinds of nondestructive testing techniques that will be considered to meet the requirements of fine ceramics was done.

As a result, on several conditions, the following possibilities are obtained. The penetration test (PT) for surface defects, the ultrasonic test (UT) and scanning acoustic microscopy (SAM) for defects close by surface, and micro focus X-ray radiography, micro focus X-ray CT for internal defects are practical and X-ray CT is especially expected to be improved.

3.2 Proof Test

43070054KKKK Tokyo FINE CERAMICS in English Mar 93 p 1965

[English abstract of article by Akihiko Suzuki and Junichi Hamanaka, Ishikawajima-Harima Heavy Industries Co., Ltd., Research Institute]

[Text] Proof testing is one of the most important technologies to assure the safety of ceramic components under thermal and mechanical loading. In this article, theoretical and experimental efforts for developing the proof-testing technology are briefly described where the results obtained in the project on Basic Technologies for Future Industries—Fine Ceramics—are mainly referred and several results selected from literature are also included. Discussions are made on the methodology for the assurance of the strength of ceramic components and the proof test is concluded to be the most convenient technique for this purpose at present. Factors which influence the effect of the proof test are made clear, and their influence is analyzed by the theory based on the Weibull statistical theory and the SCG theory and also by experimental data. A guide on how to conduct the proof test is newly proposed here on the background mentioned above, which relates to a design guide for ceramic components proposed and described in Section 3.3 of this literature. The proof-testing guide proposed here is only tentative and should be developed through experiences on actual use of ceramic components.

3.3 Design Technology for Fine Ceramic Components

3.3.1 A Design Guide for Fine Ceramic Components

43070054LLLL Tokyo FINE CERAMICS in English Mar 93 p 1997

[English abstract of article by Akihiko Suzuki and Junichi Hamanaka, Ishikawajima-Harima Heavy Industries Co., Ltd., Research Institute]

[Text] A design guide is proposed to assure the safety and reliability of fine ceramic components which operate under mechanical and thermal loads. The guide is intended to keep the fracture probability of components below a certain allowable level in the fast fracture as well as in the time-dependent fracture. This is attained by satisfying a design formula written in the guide which limits the maximum stresses of some specific sections of the components to an allowable value. The guide also provides alternate design formula for proof-tested components to assess the effect of the proof test.

3.3.2 Analysis Method for Stress and Reliability of Ceramic Components

43070054MMMM Tokyo FINE CERAMICS in English Mar 93 p 2039

[English abstract of article by Junichi Hamanaka and Akihiko Suzuki, Ishikawajima-Harima Heavy Industries Co., Ltd.]

[Text] It is important to develop the stress analysis technology of high accuracy for ceramic components because ceramics is the brittle material and the strength of ceramic components is strongly controlled by the magnitude of highly localized stress in the body. In order to evaluate the strength of ceramic components, it is also important to develop the technology for calculating the failure probability of ceramic components at given stress fields.

Here, as an example for the stress analysis technology of high accuracy, a newly developed analysis method for transient heat conduction problems is described. Also described is a reliability analysis method which is able to calculate the failure probability of ceramic components in the fast fracture mode, the static fatigue fracture mode, and the cyclic fatigue fracture mode. The method is also applicable to evaluate the failure probability of ceramic components survived proof testing.

3.4 Various Strength Testing for Ceramic Components

3.4.1 Friction and Wear of Ceramics

43070054NNNN Tokyo FINE CERAMICS in English Mar 93 p 2069

[English abstract of article by Mikio Iwasa, Yasuo Toibana, Saburo Kose, and Makoto Kinoshita, Government Industrial Research Institute, Osaka]

[Text] Ceramics are frequently used in various tribological conditions, such as solid-solid contact, in liquid or in powders. The purpose of this research is to develop accurate and simple wear testing methods, which can predict the performance of ceramics under those conditions. Five types of testing method were selected, namely, pin-on-disk, Sawin-type, Amsler-type, ball-on-disk and abrasion.

The friction and wear properties between ceramics were measured by the pin-on-disk method at a load of 1 kgf and a sliding velocity of 18 cm/sec. Silicon carbide showed the lowest friction and wear, followed by alumina. Silicon nitride was pretty high in friction and wear, so some improvement must be made for actual applications.

The Sawin-type method was convenient to appreciate the dependence of wear on sliding velocity. It was found that the wear between ceramics and also between metals increased sharply at certain velocity, but sliding between ceramics and metal showed very low wear because of the plastic deformation of the metal material. The Amsler-type method gave results qualitatively similar to the Sawin-type method.

The ball-on-disk method was found suitable for severe sliding conditions, because high rigidity of testing is maintained and wear volume is obtained not only from the weight loss but also from the shape of wear scar. When sliding against a steel ball, the silicon carbide disk showed the best wear resistance even at high velocity.

The abrasion wear of ceramics was measured using a diamond grinding wheel. The wear volume was also able to be evaluated from the shape of the wear scar shape. It was found that abrasion wear resistance was maximum for silicon nitride and minimum for alumina.

3.4.2 Thermal Shock Testing

430700540000 Tokyo FINE CERAMICS in English Mar 93 p 2089

[English abstract of article by Takao Mikami, Tadashi Sasa, Junsuke Okamura, and Kooichi Katohno, Ishikawajima-Harima Heavy Industries Co., Ltd., Research Institute]

[Text] For the realization of application of "Fine Ceramics" to mechanical parts under the environment of high temperature and corrosion, we have developed the evaluation technology and apparatuses for ceramic parts of static structural members and have evaluated model parts fabricated by the process technology group as described below.

In the second phase of this project from FY1984 to FY1987 thermal shock test equipment using an electric furnace was developed and then cylindrical model parts supplied by the process technology group were evaluated.

Finally in the third phase a thermal cycle test equipment using a combustor was developed and turbine nozzle models with complex shape in relation to a pilot turbine system from a coal gasification plant were evaluated.

As a result, we confirmed that the testing methods developed were effective to evaluate the reliability of ceramic parts under transient thermal stresses caused by thermal shock and that the objective property values were satisfied in both the cylindrical and the turbine nozzle models.

3.4.3 High Temperature Spin and Rig Test

43070054PPPP Tokyo FINE CERAMICS in English Mar 93 p 2114

[English abstract of article by J. Okamura, K. Tagashira, K. Katoono, and M. Mizuhashi, Ishikawajima-Harima Heavy Industries Co. Ltd.]

[Text] In this section some test results and their evaluation methods of ceramic rotating models are described.

This program started in 1981 as a national project of fine ceramics R&D. This project was divided into four periods.

In each period, a target value regarding material strength was set up. In the first period, cold spin tests by existing powder material have been carried out. The model shapes are shown in Figure 1 [not reproduced]. Through the tests, some valuable information was obtained, such as effect of the model's effective volume on the strength, the data obtained followed by Weibull statistics, and so on. Also by this test, the ceramic model evaluation method was established. In the second period, the turbine disk model was chosen as an evaluation named called the first model. As shown in Figure 5 [not reproduced], the target value was 30kg/mm^2 at the temperature of 1200°C. Three different material or manufacturing processes of the disk model were tested. The target value of 30kg/mm^2 was attained in every model although the Weibull modulus showed a lower value than expected. In the third period of this project, the bladed model was selected as a second model. The target value was 600MPa at 1250°C. The results were almost 80% of the target value. This is supposed to be a higher effective volume of the model. In the fourth period, the combination of the bladed disk model and the nozzle model was chosen and named the generalized test. In this test, in addition to hot spin testing, thermal shock test by igniting and shut down of a fuel [as published]. The maximum inlet temperature is 1400°C. The temperature at blade is 1250°C. Some results have been obtained by this test.

- END -

Foreign Broadcast Information Service (FBIS) and Joint Publications Research Service (JPRS) publications contain political, military, economic, environmental, and sociological news, commentary, and other information, as well as scientific and technical data and reports. All information has been obtained from foreign radio and television broadcasts, news agency transmissions, newspapers, books, and periodicals. Items generally are processed from the first or best available sources. It should not be inferred that they have been disseminated only in the medium, in the language, or to the area indicated. Items from foreign language sources are translated; those from English-language sources are transcribed. Except for excluding certain diacritics, FBIS renders personal names and place-names in accordance with the romanization systems approved for U.S. Government publications by the U.S. Board of Geographic Names.

Headlines, editorial reports, and material enclosed in brackets [] are supplied by FBIS/JPRS. Processing indicators such as [Text] or [Excerpts] in the first line of each item indicate how the information was processed from the original. Unfamiliar names rendered phonetically are enclosed in parentheses. Words or names preceded by a question mark and enclosed in parentheses were not clear from the original source but have been supplied as appropriate to the context. Other unattributed parenthetical notes within the body of an item originate with the source. Times within items are as given by the source. Passages in boldface or italics are as published.

SUBSCRIPTION/PROCUREMENT INFORMATION

The FBIS DAILY REPORT contains current news and information and is published Monday through Friday in eight volumes: China, East Europe, Central Eurasia, East Asia, Near East & South Asia, Sub-Saharan Africa, Latin America, and West Europe. Supplements to the DAILY REPORTs may also be available periodically and will be distributed to regular DAILY REPORT subscribers. JPRS publications, which include approximately 50 regional, worldwide, and topical reports, generally contain less time-sensitive information and are published periodically.

Current DAILY REPORTs and JPRS publications are listed in *Government Reports Announcements* issued semimonthly by the National Technical Information Service (NTIS), 5285 Port Royal Road, Springfield, Virginia 22161 and the *Monthly Catalog of U.S. Government Publications* issued by the Superintendent of Documents, U.S. Government Printing Office, Washington, D.C. 20402.

The public may subscribe to either hardcover or microfiche versions of the DAILY REPORTs and JPRS publications through NTIS at the above address or by calling (703) 487-4630. Subscription rates will be provided by NTIS upon request. Subscriptions are available outside the United States from NTIS or appointed foreign dealers. New subscribers should expect a 30-day delay in receipt of the first issue.

U.S. Government offices may obtain subscriptions to the DAILY REPORTs or JPRS publications (hardcover or microfiche) at no charge through their sponsoring organizations. For additional information or assistance, call FBIS, (202) 338-6735,or write to P.O. Box 2604, Washington, D.C. 20013. Department of Defense consumers are required to submit requests through appropriate command validation channels to DIA, RTS-2C, Washington, D.C. 20301. (Telephone: (202) 373-3771, Autovon: 243-3771.)

Back issues or single copies of the DAILY REPORTs and JPRS publications are not available. Both the DAILY REPORTs and the JPRS publications are on file for public reference at the Library of Congress and at many Federal Depository Libraries. Reference copies may also be seen at many public and university libraries throughout the United States.

END OF FICHE

DATE FILMED

15 JUNE 1994